chemical properties. The positive shift in potential upon formation of $Au[P(R)_3]_2^+$ may have important biological implications. For example, formation of $Au[P(C_2H_5)_3](SR)^+$ where SR is a sulfur-containing ligand such as cysteine-34 of mercaptalbumin occurs[7,8] when either $Au[P(C_2H_5)_3]Cl$ or $Au[P(C_2H_5)_3]_2^+$ is added to a matrix modeling biological systems. If the potential for the

oxidation of $Au[P(C_2H_5)_3](SR)^+$ is also significantly shifted to lower potentials, this species could become active toward redox reactions.

Contribution from the Department of Chemistry, and the LASER Laboratory, Michigan State University, East Lansing, Michigan 48824, and Laboratory of Biochemistry, University of Amsterdam, P.O. Box 20151, 1000 HD Amsterdam, The Netherlands

Factors Affecting the Iron–Oxygen Vibrations of Ferrous Oxy and Ferryl Oxo Heme Proteins and Model Compounds

W. Anthony Oertling,[†,§] Robert T. Kean,[†,‖] Ron Wever,[‡] and Gerald T. Babcock*,[†]

Resonance Raman (RR) and UV–visible absorption spectra of various imidazole-ligated ferrous oxy (Fe^{II}—O_2) and ferryl oxo (Fe^{IV}=O) porphyrins are presented. Because physiologically relevant porphyrins have been used in this study, these measurements provide a basis to identify protein-induced changes in the iron–oxygen vibrations, as well as in the structure-sensitive macrocycle vibrations and in the optical absorption spectra, of heme enzyme intermediates. The iron–oxygen stretching frequencies, $\nu(Fe^{IV}$=O), of ferryl oxo complexes of octaethylporphyrin (OEP), protoporphyrin IX dimethyl ester (PPDME), and tetraphenylporphyrin (TPP) in toluene at –120 °C reported here, together with results from other model compounds, are used to interpret the values of $\nu(Fe^{IV}$=O) reported for ferryl-oxo myoglobin and the catalytic intermediates of several peroxidase enzymes. We identify the major protein influence on the $\nu(Fe^{IV}$=O) frequency to be the trans-ligand strength of the proximal histidine, with a minor, but nonetheless important, effect being imposed by distal hydrogen bonding of the oxo ligand (Sitter, A. J.; Reczek, C. M.; Terner, J. *J. Biol. Chem.* **1985**, *260*, 7515–7522. Hashimoto, S.; Tatsuno, Y.; Kitagawa, T. *Proc. Natl. Acad. Sci. U.S.A.* **1986**, *83*, 2417–2421). This analysis follows from the inverse correlation we identify for $\nu(Fe^{IV}$=O) with respect to $\nu(Fe^{II}$=His). For the ferrous oxy complexes of OEP, protoporphyrin IX (PP), and porphyrin *a* (PA) in DMF and CH_2Cl_2 at –120 °C, the $\nu(Fe^{II}$=O_2) values we obtain are compared with similar measurements on other model compounds. As opposed to the ferryl oxo systems, in which $\nu(Fe^{IV}$=O) correlates inversely with trans-ligand strength, a direct correlation exists between $\nu(Fe^{II}$=O_2) and the strength of the iron/trans-ligand interaction in the model systems (Walters, M. A.; Spiro, T. G.; Suslick, K. S.; Collman, J. P. *J. Am. Chem. Soc.* **1980**, *102*, 6857–6858. Kerr, E. A.; Mackin, H. C.; Yu, N.-T. *Biochemistry* **1983**, *22*, 4373–4379). Moreover, we interpret the available data to indicate that $\nu(Fe^{II}$—O_2) correlates inversely with $\nu(O$=O) of bound dioxygen. We use these observations to evaluate the iron–oxygen vibrations of oxy myoglobin, horseradish peroxidase compound III, and an early intermediate in the reduction of O_2 by cytochrome *c* oxidase; we conclude that the iron–oxygen stretching frequencies displayed by the various ferrous oxy proteins can be understood in terms of distal influences on the electron density in the O=O bond.

Introduction

Two intermediates of considerable interest in reactions catalyzed by heme proteins are ferrous oxy (Fe^{II}—O_2) and ferryl oxo (Fe^{IV}=O) compounds. The ferrous oxy species is exemplified by hemoglobin and myoglobin, which bind O_2 reversibly when the heme is in a ferrous state. The initial intermediate in the reduction of dioxygen by cytochrome *c* oxidase[1] is a ferrous oxy compound,[2,3] and a ferrous oxy species has been identified as a reaction intermediate of cytochrome P-450.[4] Dioxygen binding can also be easily induced in ferrous peroxidase samples to produce a ferrous oxy species (compound III), which can, alternatively, be formed by the addition of excess H_2O_2 to the ferric enzyme.[5] Ferryl oxo species have been postulated in the catalytic cycle of cytochrome *c* oxidase,[6] as the oxygen-donating species in cytochrome P-450,[7] and as intermediates in the reactions of catalases and peroxidases.[8] Addition of peroxide to the normally unreactive globin hemes can also induce the formation of ferryl species.[9] The variation in reactivity and catalytic function of both ferrous oxy and ferryl oxo species in different proteins suggests protein variations in the heme vicinity. Identification of these protein differences should provide considerable insight into the catalytic mechanisms of these proteins.

Resonance Raman spectroscopy (RR) has the resolution necessary to probe these protein-specific structural variations and has

been applied to ferrous oxy heme proteins.[10-15] Recently Varotsis et al.[3] have used two-color, time-resolved RR measurements of

---

† Michigan State Unversity.
‡ University of Amsterdam.
§ Present address: INC-4, Mail Stop C-345, Los Alamos National Laboratory, Los Alamos, NM 87545.
‖ Present address: Cargill Inc., Research Division, P.O. Box 9300, Minneapolis, MN 55440.

(1) (a) Wikstrom, M.; Krab, K.; Saraste, M. *Cytochrome Oxidase, A Synthesis*; Academic Press: New York, 1981. (b) Naqui, A.; Chance, B. *Annu. Rev. Biochem.* **1986**, *55*, 137–166. (c) Hill, B. C.; Greenwood, C.; Nicholls, P. *Biochim. Biophys. Acta* **1986**, *853*, 91–113. (d) Chan, S. I.; Witt, S. N.; Blair, D. F. *Chem. Scr.* **1988**, *28A*, 51–58. (e) Babcock, G. T. In *Biological Applications of Raman Spectroscopy*; Spiro, T. G., Ed.; Wiley: New York, 1988; pp 293–346.
(2) (a) Babcock, G. T.; Jean, J. M.; Johnston, L. N.; Palmer, G.; Woodruff, W. H. *J. Am. Chem. Soc.* **1984**, *106*, 8305–8306. (b) Babcock, G. T.; Jean, J. M.; Johnston, L. N.; Woodruff, W. H.; Palmer, G. *J. Inorg. Biochem.* **1985**, *23*, 243–251.
(3) (a) Varotsis, C.; Woodruff, W. H.; Babcock, G. T. *J. Am. Chem. Soc.* **1989**, *111*, 6439–6440; *J. Am. Chem. Soc.* **1990**, *112*, 1297. (b) Varotsis, C.; Woodruff, W. H.; Babcock, G. T. *J. Biol. Chem.*, in press.
(4) (a) Peterson, J. A. *Biochem. Biophys. Res. Commun.* **1971**, *42*, 140–142. (b) Bangcharoenpaurpong, O.; Rizos, A.; Champion, P. M.; Jollie, D.; Sligar, S. *J. Biol. Chem.* **1986**, *261*, 8089–8092.
(5) (a) Keilin, D.; Mann, T. *Proc. R. Soc. London, B* **1937**, *122*, 119–133. (b) Wittenberg, J. B.; Noble, R. W.; Wittenberg, B. A.; Antonini, E.; Brunori, M.; Wyman, J. *J. Biol. Chem.* **1967**, *242*, 626–634. (c) Nakajima, Ryo; Yamazaki, I. *J. Biol. Chem.* **1987**, *262*, 2576–2581.
(6) (a) Wikstrom, M. *Proc. Natl. Acad. Sci. U.S.A.* **1981**, *78*, 4051–4054. (b) Blair, D. F.; Witt, S. N.; Chan, S. I. *J. Am. Chem. Soc.* **1985**, *107*, 7389–7399.
(7) Groves, J. T. In *Cytochrome P-450: Structure, Mechanism and Biochemistry*; Ortiz de Montellano, P., Ed.; Plenum Press: New York, 1986; Chapter 1.
(8) (a) Dunford, H. B. *Adv. Inorg. Biochem.* **1982**, *4*, 41–68. (b) Few, J. E.; Jones, P. In *Advances in Inorganic and Bioinorganic Mechanism*; Academic Press: New York, 1984; Vol. 3, pp 175–212.
(9) (a) George, P.; Irvine, D. H. *Biochem. J.* **1952**, *52*, 511–517. (b) Uyeda, M.; Peisach, J. *Biochemistry* **1981**, *20*, 2028–2035.
(10) Brunner, H. *Naturwissenschaften* **1974**, *61*, 129.
(11) Duff, L. L.; Applemen, E. H.; Shriner, D. F.; Klotz, I. M. *Biochem. Biophys. Res. Commun.* **1979**, *90*, 1098–1103.

flowing samples prepared by rapid mixing to identify an oxygen isotope sensitive vibration in an early intermediate (most likely a ferrous oxy complex) in the reaction of bovine cytochrome *c* oxidase (Cyt Ox) with dioxygen. RR measurements have also been used to identify and characterize several ferryl oxo proteins.[16–21] An important observation that has emerged from this work is that the ferryl oxo stretching frequencies vary significantly between different protein species and from those of the models that have been prepared thus far, whereas the ferrous oxy frequencies are, except for a single example, largely constant in a number of different protein environments (see tables below). This is somewhat surprising, given the definite trends in $\nu(Fe^{II}O_2)$ recognizable in the model compounds and the diverse functions of the various proteins.

Ferrous oxy[22–25] and ferryl oxo[26–30] porphyrin model compounds have been studied by Raman spectroscopy in order to investigate the origins of the in situ behavior of the oxygenated complexes. Owing to the complexity of the synthetic procedures and to the inherent instability of these compounds, however, most of the model compounds used to date fail to reproduce one or more of the basic structural features of the protein-bound chromophore. For example, porphyrins substituted at the methine carbons have been used extensively in these experiments, and oftentimes five-coordinate states of the iron, rather than the six-coordinate states that normally occur in situ, have been studied. To address this situation, we have recently developed techniques by which Raman and optical absorption spectra of oxy and oxo complexes of naturally occurring iron porphyrins may be obtained.[31] In the
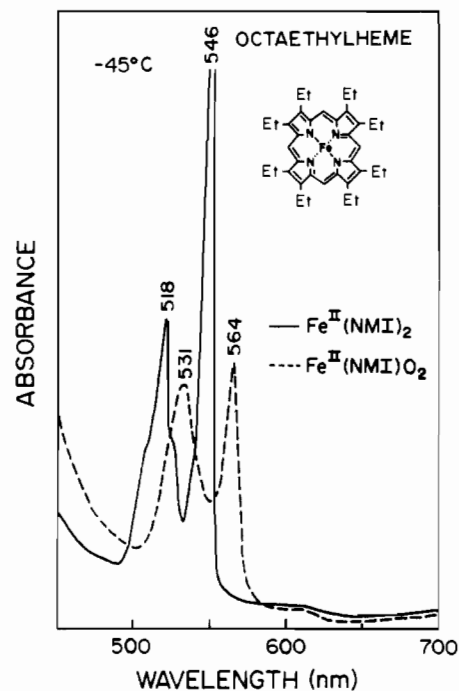

Figure 1. Visible absorption of spectra of DMF solutions of 0.5 mM six-coordinate ferrous octaethylporphyrin complexes in EPR tubes at −45 °C. The ordinate scale is not quantified, owing to the background absorbance of the low-temperature apparatus.

work reported here, we have used these techniques to study several six-coordinate ferrous oxy and ferryl oxo heme model compounds. 1-Methylimidazole (NMI) was used as the sixth ligand to model the usual occurrece of histidine in the trans axial position in the protein systems. Complexes of octaethylporphyrin, protoporphyrin IX, and porphyrin *a* were used for the ferrous oxy models, and complexes of octaethylporphyrin, protoporphyrin IX dimethyl ester, and tetraphenylporphyrin were used for the ferryl oxo models. By the establishment of the solution spectral properties of the unperturbed chromophores, the results of these studies provide insights into the nature of protein–heme interactions in ferrous oxy and ferryl oxo heme proteins. In the present work, we use these new model compound results, in conjunction with model compound and protein data collected to date, to analyze the environmental effects likely to be responsible for the variation of the iron–oxygen vibrations of myoglobin, various peroxidases, and cytochrome *c* oxidase.

Materials and Methods

Methylene chloride was dried by reflux over calcium hydride prior to use. Toluene was distilled from sodium benzophenone ketyl. Toluene-d_8 (Cambridge Isotope Laboratories) was dried over molecular sieves (4 and 5 Å) and used without further purification. Dimethylformamide (DMF) was vacuum distilled over calcium hydride. Sodium dithionite (a gift from Virginia Chemical Inc.) and tetrabutylammonium borohydride (TBAB, from Aldrich) were stored in vacuum desiccators and used without further purification. Iron protoporphyrin IX (FePP, Sigma, bovine hemin) was used without further purification for preparation of the oxy models. Iron protoporphyrin IX dimethylester (FePPDME), iron tetraphenylporphyrin (FeTPP), and iron octaethylporphyrin (FeOEP) were prepared from free-base porphyrins (Porphyrin Products). Iron porphyrin *a* (FePA) was isolated from bovine heart cytochrome *c* oxidase as previously described.[32]

The procedures for the preparation of the oxy porphyrin complexes, $(NMI)Fe^{II}–O_2$, were based on those reported earlier.[33] Solutions of the

(12) (a) Nagai, K.; Kitagawa, T.; Morimoto, H. *J. Mol. Biol.* **1980**, *136*, 271–289. (b) Tsubaki, M.; Nagai, K.; Kitagawa, T. *Biochemistry* **1980**, *19*, 379–385.

(13) (a) Tsubaki, M.; Yu, N.-T. *Proc. Natl. Acad. Sci. U.S.A.* **1981**, *78*, 3581–3585. (b) Kerr, E. A.; Yu, N.-T.; Bartnicki, D. E.; Mizukami, H. *J. Biol. Chem.* **1985**, *260*, 8360–8565.

(14) (a) Walters, M. A.; Spiro, T. G. *Biochemistry* **1982**, *21*, 6989–6995. (b) Walters, M. A.; Spiro, T. G.; Scholler, D. M.; Hoffman, B. H. *J. Raman Spectrosc.* **1983**, *14*, 162–165.

(15) VanWart, H. E.; Zimmer, J. *J. Biol. Chem.* **1985**, *260*, 8372–8377.

(16) (a) Terner, J.; Sitter, A. J.; Reczek, C. M. *Biochem. Biophys. Acta* **1985**, *828*, 73–80. (b) Sitter, A. J.; Reczek, C. M.; Terner, J. *Biochem. Biophys. Acta* **1985**, *828*, 229–235. (c) Reczek, C. M.; Sitter, A. J.; Terner, J. *J. Mol. Struct.*, in press.

(17) (a) Hashimoto, S.; Tatsuno, Y.; Kitagawa, T. *Proc. Jpn. Acad., Sec. B* **1984**, *60*, 345–348. (b) Hashimoto, S.; Teraoka, J.; Inubushi, T.; Yonetani, T.; Kitagawa, T. *J. Biol. Chem.* **1986**, *261*, 11110–11118.

(18) Makino, R.; Uno, T.; Nishimura, Y.; Iizuka, T.; Tsuboi, M.; Ishimura, Y. *J. Biol. Chem.* **1986**, *261*, 8376–8382.

(19) Oertling, W. A.; Babcock, G. T. *Biochemistry* **1988**, *27*, 3331–3338.

(20) Oertling, W. A.; Hoogland, H.; Babcock, G. T.; Wever, R. *Biochemistry* **1988**, *27*, 5395–5400.

(21) (a) Paeng, K.-J.; Kincaid, J. R. *J. Am. Chem. Soc.* **1988**, *110*, 7913–7915. (b) Terner, J. Unpublished results.

(22) (a) Burke, J. M.; Kincaid, J. R.; Peters, S.; Gagne, R. R.; Collman, J. P.; Spiro, T. G. *J. Am. Chem. Soc.* **1978**, *100*, 6083–6087. (b) Walters, M. A.; Spiro, T.; Suslick, K. S.; Collman, J. P. *J. Am. Chem. Soc.* **1980**, *102*, 6857–6858.

(23) (a) Kerr, E. A.; Mackin, H. C.; Yu, N.-T. *Biochemistry* **1983**, *22*, 4373–4379. (b) Yu, N.-T.; Mackin Thompson, H. C.; Chang, C. K. *Biophys. J.* **1987**, *51*, 283–287.

(24) (a) Wagner, W.-D.; Paeng, I. R.; Nakamoto, K. *J. Am. Chem. Soc.* **1988**, *110*, 5565–5567. (b) Nakamoto, K.; Paeng, I. R., Kuroi, T.; Isobe, T.; Oshio, H. *J. Mol. Struct.* **1988**, *189*, 293–300.

(25) Desbois, A.; Momenteau, M.; Lutz, M. *Inorg. Chem.* **1989**, *28*, 825–834.

(26) (a) Bajdor, K.; Nakamoto, K. *J. Am. Chem. Soc.* **1984**, *106*, 3045–3046. (b) Proniewicz, L. M.; Bajdor, K.; Nakamoto, K. *J. Phys. Chem.* **1986**, *90*, 1760–1766.

(27) (a) Schappacher, M.; Chottard, G.; Weiss, R. *J. Chem. Soc., Chem. Commun.* **1986**, 93–94. (b) Gold, A.; Jayaraj, K.; Doppelt, P.; Weiss, K.; Chottard, G.; Bill, E.; Ding, X.; Trautwein, A. X. *J. Am. Chem. Soc.* **1988**, *110*, 5756–5761.

(28) Czernuszewicz, R. S.; Macor, K. A. *J. Raman Spectrosc.* **1988**, *19*, 553–557.

(29) Hashimoto, S.; Tatsuno, Y.; Kitagawa, T. *J. Am. Chem. Soc.* **1987**, *109*, 8096–8097.

(30) Kincaid, J. R.; Schneider, A. J.; Paeng, K.-J. *J. Am. Chem. Soc.* **1989**, *111*, 735–737.

(31) Kean, R. T.; Oertling, W. A.; Babcock, G. T. *J. Am. Chem. Soc.* **1987**, *109*, 2185–2187.

(32) Babcock, G. T.; Vickery, L. E.; Palmer, G. *J. Biol. Chem.* **1976**, *251*, 7907–7919.

(33) (a) Brinigar, W. S.; Chang, C. K. *J. Am. Chem. Soc.* **1974**, *96*, 5595–5597. (b) Wagner, G. C.; Kassner, R. J. *J. Am. Chem. Soc.* **1974**, *96*, 5593–5595. (c) Babcock, G. T.; Chang, C. K. *FEBS Lett.* **1979**, *97*, 358–362.
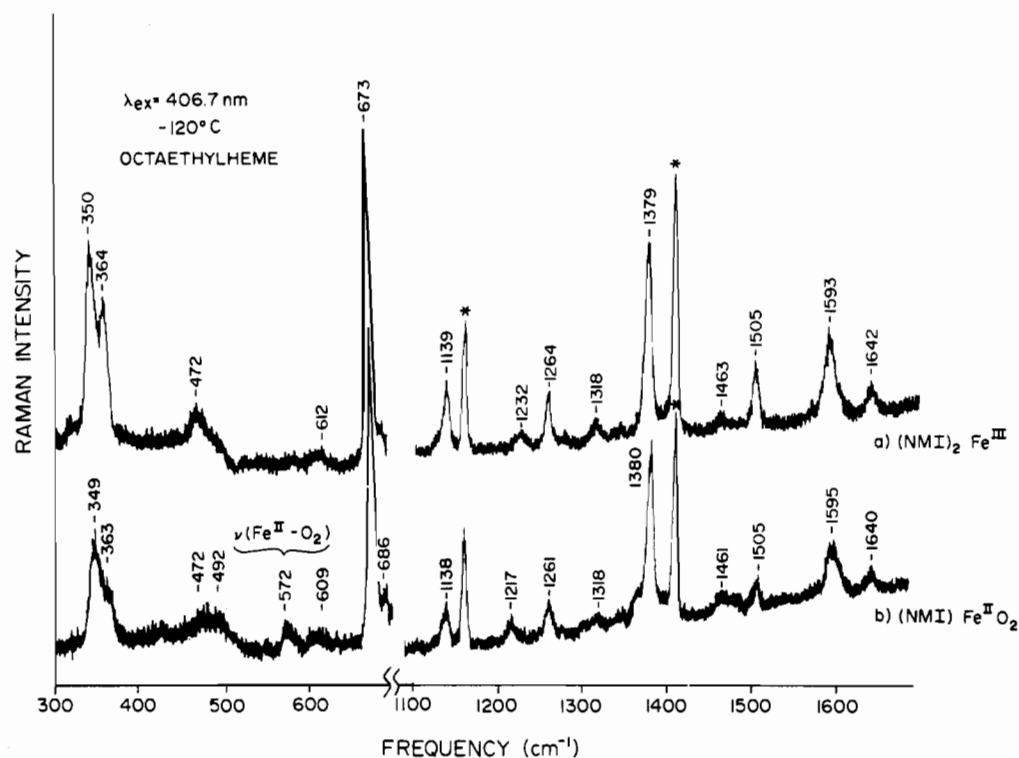
Figure 2. Soret enhanced resonance Raman spectra of frozen CH_2Cl_2 solutions of 0.3 mM six-coordinate octaethylporphyrin complexes at -120 °C. Low-frequency spectra were obtained by a single scan at a rate of 10 cm^{-1}/min. High-frequency spectra represent one scan at 50 cm^{-1}/min. Solvent peaks are labeled with an asterisk. Laser power at 406.7 nm was 15 mW.

various hemes ($\sim$50–250 μM) were prepared in methylene chloride or DMF that contained an $\sim$100-fold excess of NMI. These were then purged of oxygen in Schlenk-line glassware by using several freeze-pump–thaw cycles. A positive pressure of argon gas was maintained over the sample during the thaw stages. $(NMI)_2Fe^{III}(OEP)Cl$ in methylene chloride was reduced to $(NMI)_2Fe^{II}OEP$ by the addition of a slight excess of solid TBAB. The ferric porphyrins in DMF were reduced by titration with a degassed aqueous dithionite solution. These reductions were monitored by using optical absorption spectroscopy. Oxygen binding was achieved by the addition of oxygen to the cooled samples (-45 to -70 °C) with a gastight syringe. Binding was monitored optically (see below) and shown to be reversible by displacement of the O_2 with CO followed by degassing under strong illumination.[33]

Preparation of the ferryl oxo porphyrins, $(NMI)Fe^{IV}=O$, was performed according to the procedure developed by Balch and co-workers,[34] with the exception that the anaerobic steps were carried out in Schlenk-line glassware instead of an anaerobic glovebox. The procedure worked well for the FePPDME in addition to the FeOEP and FeTPP. Use of the non-esterified protoheme was prohibited by its negligible solubility in toluene. Isotopic labeling of both the ferrous oxy and ferryl oxo compounds was achieved by the use of $^{18}O_2$ (98% Cambridge Isotope Laboratories) in the respective synthetic procedures.

The peroxidase species used to record the spectra in Figure 8 were prepared by following procedures given in our previous work on these enzymes.[20]

Optical absorption spectra were obtained with a Perkin–Elmer Lamda 5 UV–visible spectrophotometer. Low-temperature optical absorption spectra were obtained by using a house-built optical Dewar.[35a] The samples were contained in EPR tubes, which were cooled to the desired temperature by flowing cold nitrogen gas. Raman spectra were obtained with a Spex 1401 scanning monochromator equipped with an RCA 31034C PMT detector by using 15-mW incident laser power at 406.7 nm (Spectra-Physics Model 164 Kr ion laser) in a backscattering geometry. The samples in EPR tubes were spun continuously during laser irradiation in a similar low-temperature Dewar designed specifically for the

(34) (a) Chin, D.-H.; Balch, A. L.; La Mar, G. N. *J. Am. Chem. Soc.* **1980**, *102*, 1446–1448. (b) Chin, D.-H.; La Mar, G. N.; Balch, A. L. *J. Am. Chem. Soc.* **1980**, *102*, 4344–4350. (c) La Mar, G. N.; deRopp, J. S.; Latos-Grazynski, L.; Balch, A. L.; Johnson, R. S.; Smith, K. B.; Parish, D. W.; Cheng, R. J. *J. Am. Chem. Soc.* **1983**, *105*, 782–787.
(35) (a) Kean, R. T. Ph.D. Dissertation, Michigan State University, 1987. (b) Oertling, W. A.; Babcock, G. T. *J. Am. Chem. Soc.* **1985**, *107*, 6406–6407.

Table I. Optical Absorption Maxima (nm) of Ferrous Oxy and Ferryl Oxo Porphyrins and Heme Proteins

	abs max		
model	Soret	visible[a]	solvent; temp
$(NMI)_2Fe^{II}OEP$	413	517 < 545	CH_2Cl_2; 80 °C
$(NMI)_2Fe^{III}OEP$	403	524 > 552	CH_2Cl_2; room temp
$(NMI)Fe^{II}$—$O_2(OEP)$	404	530 = 563	CH_2Cl_2; −80 °C
$(NMI)Fe^{II}$—$O_2(OEP)$	404	531 = 564	DMF; −45 °C
$(NMI)Fe^{II}$—$O_2(PP)$	415	540 = 574	DMF; −45 °C
$(NMI)Fe^{II}$—$O_2(PA)$	426	579 < 595	DMF; −45 °C
$(NMI)Fe^{IV}=O(OEP)$	406	535, 546 = 573	toluene; −90 °C
$(NMI)Fe^{IV}=O(PPDME)$	416	543, 555 = 584	toluene; −90 °C
$(NMI)Fe^{IV}=O(TPP)$	427	555, 563 > 597	toluene; −90 °C

[a] <, >, or = reflects relative intensities of the absorptions at the wavelength listed.

Raman measurement.[35] A linear, sloping background was subtracted from some Raman spectra, as indicated in the figure captions, but no smoothing was done.

Results

Ferrous Oxy Species. The optical absorption spectra of the ferrous complexes $(NMI)_2Fe^{II}OEP$ and $(NMI)Fe^{II}$—$O_2(OEP)$ are shown in Figure 1. As expected, the latter is similar to that reported for six-coordinate, ferrous oxy mesoporphyrin, and the absorption spectra of the six-coordinate ferrous oxy complexes of protoporphyrin IX and porphyrin a (not shown) are in agreement with previously reported spectra.[33] The absorption maxima that we measure for these and other complexes are listed in Table I. As seen from the absorption spectra in Figure 1, the formation of the $(NMI)Fe^{II}$–O_2 species from the $(NMI)_2Fe^{II}$ species is accompanied by a red shift of the α and β bands and a change in their intensities. The Soret maximum blue shifts to a value close to that of the corresponding $(NMI)_2Fe^{III}$ compound (see Table I). This behavior was observed for all of the porphyrin complexes used in these experiments.

The RR spectrum of $(NMI)_2Fe^{III}OEP$ is typical of those for low-spin ferri hemes and is displayed in Figure 2. However, the spectrum of $(NMI)Fe^{II}$–$O_2(OEP)$, also shown in Figure 2, is *not* typical of those for low-spin ferrous hemes.[36] Indeed, the

Table II. Structure-Sensitive Resonance Raman Frequencies (cm⁻¹) of Ferrous Oxy and Ferryl Oxo Porphyrins and Heme Proteins[a]

model	ν_{10}	ν_2	ν_3	ν_4	ref
$(NMI)_2Fe^{III}(OEP)$	1642	1592	1505	1379	this work
$(NMI)Fe^{II}—O_2(OEP)$	1640	1595	1505	1380	this work
$(NMI)Fe^{IV}=O(OEP)$	1643	~1603[b]	1506	1385	this work
$Fe^{IV}=O(OEP)$	1643	1598	1507	1379	26b
$(NMI)_2Fe^{III}(PP)$	1640	1579	1502	1373	47c
$(NMI)_2Fe^{II}—O_2(PP)$	1642	1579	1505	1374	this work
$(NMI)_2Fe^{IV}=O(PPDME)$	1642	~1586[b]	1508	1380	this work
protein					
Hb—O₂	1640	1583	1506	1377	38c
Mb—O₂	1640	1583	1505	1375	15
HRP-III	1639	1581	1506	1377	15
LPO-III	1641	1575	1504	1373	this work
MPO-III	1636		~1500 (w)	1371	this work
Mb=O	1642	1589	1513	1381	16b
HRP-II	1640	1583	1508	1379	17a, 19, 20
LiP-II	1642		1503	1379	49a
CcP-I	1640	1584	1508	1377	16c, 17b
LPO-II	1641	1578	1506	1376	this work, 16c, 49b
MPO-II	1636		~1497 (w)	1372	this work, 20

[a] Abbreviations: HRP-III and HRP-II, horseradish peroxidase compounds III and II, respectively; LiP-II, lignin peroxidase compound II; CcP-I, cytochrome *c* peroxidase compound I or ES. [b] These features were overlapped by solvent vibrations.

wavenumbers of the structure-sensitive RR bands of the ferrous oxy derivative show a strong homology to those of the bis(imidazole) ferric species (see Table II). This implies that the porphyrin geometry[37] and $e_g(\pi^*)$ orbital occupancy are remarkably similar for these two complexes despite the formal iron valence states of +2 and +3. These spectral similarities have been discussed in much detail, particularly with regard to the nature of the $Fe^{II}—O_2$ bond.[38] The $\nu(Fe^{II}—O_2)$ vibration occurs at 572–573 cm⁻¹ in the ferrous oxy compound and is absent in the spectrum of the $(NMI)_2Fe^{III}$ species. This assignment is confirmed by the shift to 547 cm⁻¹ upon substitution of $^{16}O_2$ by $^{18}O_2$ (Figure 3a,b). The frequency shift of 26 cm⁻¹ is in agreement with the value predicted by using a harmonic oscillator model. Peaks observed at 573 and 576 cm⁻¹ in the protoheme and heme *a* spectra (Figure 3) also demonstrate a 26-cm⁻¹ downshift upon $^{18}O_2$ substitution (not shown) and are likewise assigned to $\nu(Fe^{II}—O_2)$.

The expected bending vibration of the ferrous oxy moiety, $\delta(FeOO)$, has not been observed to date in Raman spectra of heme complexes; however, Bajdor et al.[39] observed two oxygen isotope sensitive bands in the RR spectrum of ferrous oxy phythalocyanate by using 676.4-nm excitation. Their normal coordinate analysis results support the original assignment made by Brunner[10] of the ~570-cm⁻¹ vibration to the iron–oxygen symmetric stretch.

Our experiments were complicated by the formation of fluorescent heme decomposition products in DMF. The fluorescence is more pronounced at low temperature, and it often obscured the high-frequency region of the Raman spectra. It also produced a sloping background in the low-frequency region that was subtracted from the data in Figure 3. The protoheme and heme *a* samples were more susceptible to the formation of fluorescent products. Despite this complication, we were able to measure the structure-sensitive vibrations in the 1300–1700-cm⁻¹ region for the $(NMI)Fe^{II}—O_2$ (PP) sample in DMF at −125 °C. These are listed in Table II along with the vibrational frequencies of analogous OEP complexes in CH_2Cl_2. These wavenumber values are of interest in order to evaluate macrocycle distortions that may
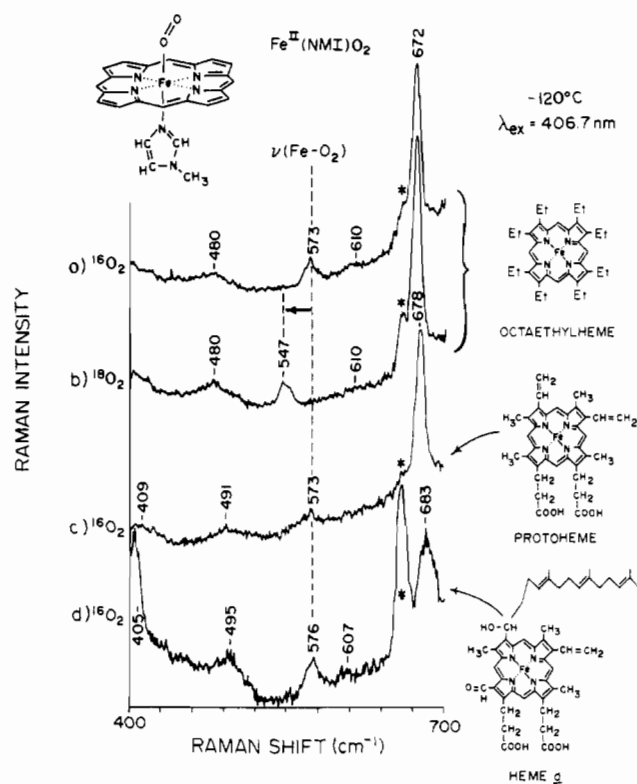

Figure 3. Low-frequency resonance Raman spectra of frozen DMF solutions of 0.5 mM six-coordinate ferrous oxy hemes at −120 °C. Linear backgrounds were subtracted from all spectra in order to remove sloping base lines caused by fluorescence. Solvent peaks are labeled with an asterisk. Spectra were accumulated from multiple runs, each acquired by stepwise scanning at 1 cm⁻¹ intervals. Laser power at 406.7 nm was 15 mW. Plots a–d are for 30 scans at 1 s/cm⁻¹.

occur in ferrous oxy heme proteins.[25]

Ferryl Oxo Species. The optical absorption spectra of the $(NMI)Fe^{IV}=O$ complexes of OEP, PPDME, and TPP are displayed in Figure 4, and the maxima appear in Table I. There is a progressive red shift in the spectra in going from OEP to PPDME to TPP, which reflects the increasing electron-withdrawing ability of the respective ring substituents. The shoulder at ~619 nm in the spectrum of the ferryl oxo PPDME sample is due to a μ-oxo dimer impurity $((PPDME)Fe)_2O$, which is the final product of autooxidation. The occurrence of this species (Soret maximum ~400 nm) also accounts for the broadness of

(36) Spiro, T. G.; Strong, J. D.; Stein, P. *J. Am. Chem. Soc.* **1979**, *101*, 2648–2655.

(37) (a) Spaulding, L. D.; Chang, C. C.; Yu, N. T.; Felton, R. H. *J. Am. Chem. Soc.* **1975**, *97*, 2517–2525. (b) Parthasarathi, N.; Hansen, C.; Yamaguchi, S.; Spiro, T. G. *J. Am. Chem. Soc.* **1987**, *109*, 3865–3871.

(38) (a) Weiss, J. J. *Nature* **1964**, *202*, 83–84. (b) Yamamoto, T.; Palmer, G.; Gill, D.; Salmeen, I. T.; Rimai, L. *J. Biol. Chem.* **1973**, *248*, 5211–5213. (c) Spiro, T. G.; Strekas, T. C. *J. Am. Chem. Soc.* **1974**, *96*, 338–345. (d) Kitagawa, T.; Kyogohu, Y.; Iizuka, T.; Ikeda-Saito, M. *J. Am. Chem. Soc.* **1976**, *98*, 5169–5172.

(39) Bajdor, K.; Oshio, H.; Nakamoto, K. *J. Am. Chem. Soc.* **1984**, *106*, 7273–7274.
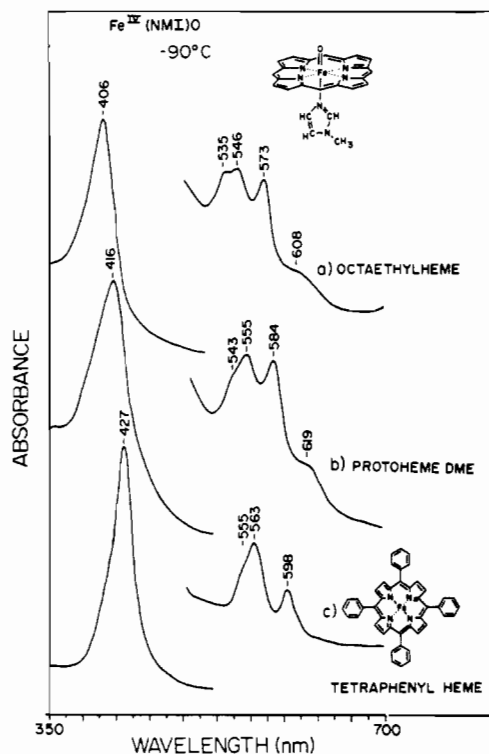
Figure 4. Optical absorption spectra of toluene solutions of 0.1 mM six-coordinate ferryl oxo hemes at −90 °C. The low-energy shoulders at 608 nm in part a and 619 nm in part b are due primarily to 10–20% μ-oxo dimer in the preparations as discussed in the text. The visible region is expanded 5-fold with respect to the Soret region of the spectrum.
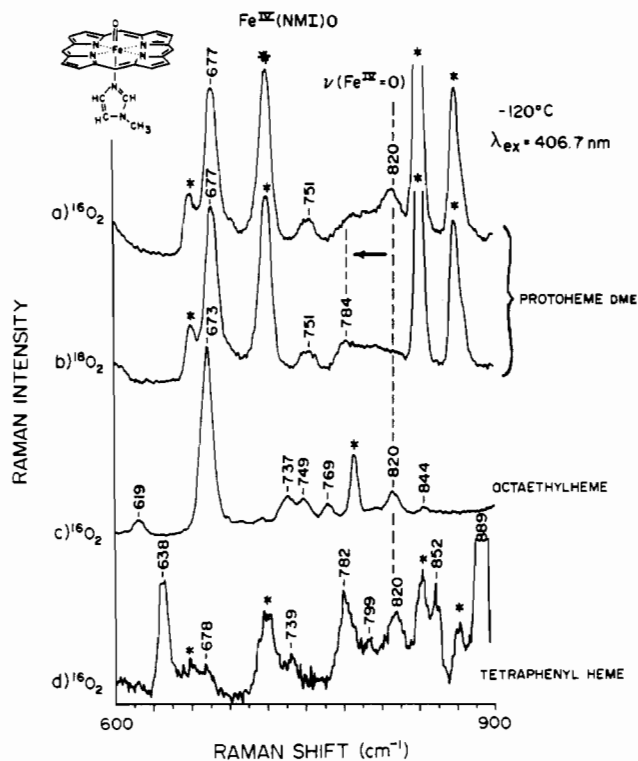

Figure 5. Low-frequency resonance Raman spectra of frozen toluene solutions of six-coordinate ferryl oxo hemes at −120 °C. Toluene-d_8 was used for plots a, b, and d. Sample concentrations were 0.1 mM for protoheme dimethyl ester, 0.4 mM for octaethylheme, and 0.8 mM for tetraphenylheme. Linear base lines were subtracted from all spectra. Solvent peaks are labeled with an asterisk. Spectra were accumulated in a manner similar to those in Figure 3. Key (a and b) five scans at 2 s/cm^{-1}; (c) five scans at 2 s/cm^{-1}; (d) two scans at 3 s/cm^{-1}.

the Soret absorption relative to the other samples, and the observed maximum may be slightly blue shifted relative to that of a pure
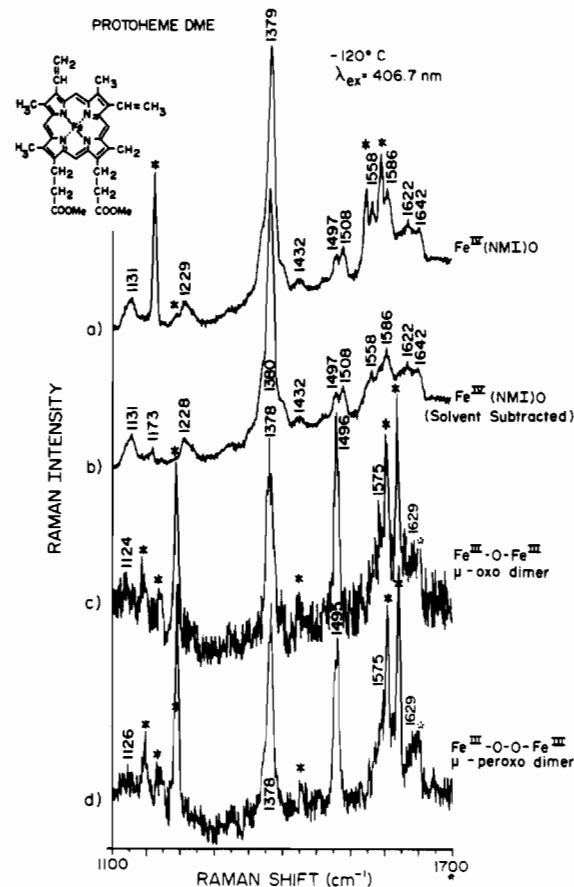

Figure 6. High-frequency resonance Raman spectra of frozen toluene solutions of protoheme dimethyl ester complexes at −120 °C. Toluene-d_8 was used for parts a and b. Sample concentrations were 0.1 mM for the ferryl oxo complex and 0.5 mM for the μ-oxo and μ-peroxo complexes. Linear base lines were subtracted from all spectra. Solvent peaks are labeled with an asterisk. Spectra were accumulated as those in Figures 3 and 5. Key (a) three scans at 2 s/cm^{-1}; (c) one scan at 2 s/cm^{-1}; (d) two scans at 2 s/cm^{-1}. The feature at 1497 cm^{-1} in parts a and b is from the μ-oxo dimer.

sample. The UV–visible absorption maxima of (NMI)Fe^{IV}=O-(PPDME) are of particular interest, as they can be compared to optical spectra of ferryl oxo derivatives of protoheme-containing proteins, e.g., compound II intermediates of heme peroxidases. A survey[35a] of the spectra of these enzyme transients shows that several display blue-shifted or red-shifted absorptions compared to the model. On the other hand, the spectrum of ferryl oxo myoglobin[9] (Mb=O) is very similar to Figure 4b. Thus, the UV–visible spectral measurement presented here provides a basis to evaluate the spectra of the protein species. Identification of the protein influences causing the spectral changes displayed by the ferryl oxo enzyme intermediates will be most informative.

In Figure 5a, we show the 600–900-cm^{-1} region of the Raman spectrum of (NMI)Fe^{IV}=O(PPDME). The peak at 820 cm^{-1} shifts to 784 cm^{-1} (Figure 5b) upon substitution of ^{16}O by ^{18}O and is assigned to the Fe^{IV}=O stretching vibration. The 36-cm^{-1} shift is expected for a ferryl oxo structure. The ν(Fe^{IV}=O) value was temperature independent over the −90 to −190 °C range; however, the intensity of this feature decreased at higher temperature, suggestive of sample decomposition. This vibration is also observed at 820 cm^{-1} in the spectra of OEP and TPP complexes in Figure 5, and it likewise exhibits a 36-cm^{-1} shift upon ^{18}O substitution (not shown) for these compounds.

In Figure 6, the high-frequency Raman spectra recorded at −120 °C for the ferryl oxo, μ-oxo, and μ-peroxo species of PPDME are presented. A solvent-subtracted spectrum of the ferryl species allows better observation of the 1550–1700-cm^{-1} region and is presented in Figure 6b. The 1497-cm^{-1} band in Figure 6a,b arises from the μ-oxo dimer contamination. The spectra of the μ-peroxo and μ-oxo species are shown in parts c and d of Figure 6 and are

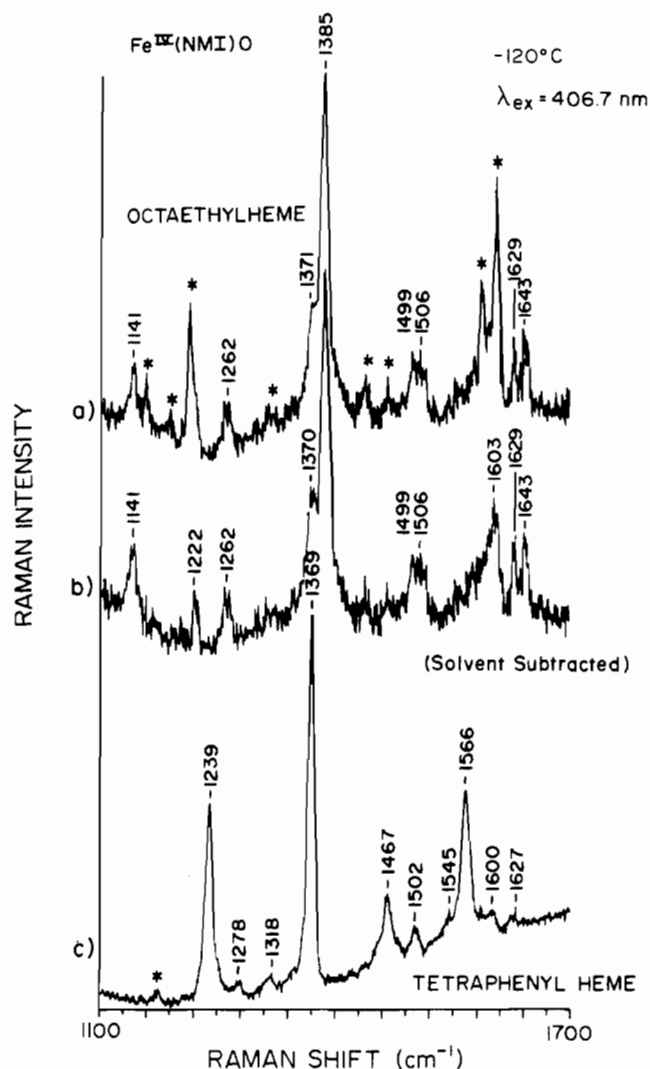**Figure 7.** High-frequency resonance Raman spectra of frozen-toluene solutions of six-coordinate ferryl oxo hemes at −120 °C. Toluene-d_8 was used for part c. Sample concentration was 0.3 mM for parts a and b and 0.8 for part c. Linear base lines were subtracted from all spectra. Solvent peaks are labeled with an asterisk. Spectra were accumulated as those in Figures 3, 5, and 6. Key (a and b) sum of two scans, the first at 1 s/cm⁻¹, the second at 2 s/cm⁻¹; (c) two scans at 2 s/cm⁻¹.

nearly identical. It is not clear whether this reflects similar electronic structures for the two species or whether the μ-peroxo complex is photolabile and rapidly decomposes to a μ-oxo complex in the laser beam.[40] Since we do not observe any variation of the spectrum with time, even in quick scans with fresh samples, we believe that the μ-peroxo heme is stable under the conditions used for data collection and that the former explanation is more probable.

In Figure 7, the high-frequency Raman scattering from $(NMI)Fe^{IV}=O(OEP)$ is presented. A solvent-subtracted spectrum is also included (Figure 7b). Spectral contributions from the μ-oxo species are evident (cf., at 1499 and 1629 cm⁻¹), as was the case with the PPDME complexes. In Figure 7c, the high-frequency Raman spectrum of $(NMI)Fe^{IV}=O$ (TPP) at −120 °C is shown.

As mentioned above, the high-frequency RR-active vibrations of the protoporphyrin model complexes are of interest because they allow identification of protein-induced distortions in the protoheme chromophores in many of the high-valent protein species. This was not possible with previous data from ferrous oxy and ferryl oxo models because porphyrins substituted at the methine carbons were typically used.[22-30] The methine substituents

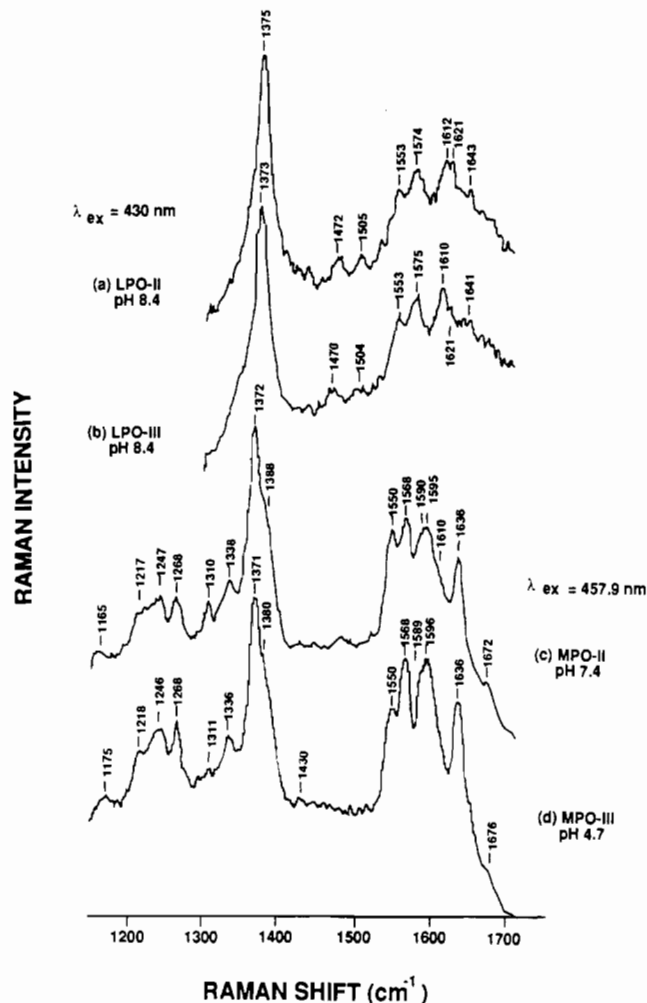(40) Paeng, I. R.; Shiwaku, H.; Nakamoto, K. *J. Am. Chem. Soc.* **1988**, *110*, 1996–1997.

Figure 8. High-frequency resonance Raman spectra of solutions of ferryl oxo (compound II) and ferrous oxy (compound III) peroxidase intermediates at 5 °C prepared under the following conditions: (a) 24 μM lactoperoxidase (LPO) in 100 mM Tris–sulfate buffer + 0.3 mM H_2O_2; (b) the same as in part a but 3.0 mM H_2O_2 added; (c) 30 μM myeloperoxidase (MPO) in 250 mM phosphate buffer + two successive additions of 0.3 mM H_2O_2; (d) 30 μM MPO in 250 mM acetate buffer + 2.5 mM H_2O_2. For further details of the enzyme preparations, see ref 50. For details of the laser Raman equipment and protocol, see refs 19 and 20. The broad feature centered at ∼1488 cm⁻¹ in part c has contributions from both ν_3 of MPO-II (∼1497 cm⁻¹, w) and ν_3 of the native MPO (∼1482 cm⁻¹, m) due to a small amount of the native form in the preparation. No other spectral features of the starting material are obvious.

of these synthetic porphyrins stabilized the oxygen adducts significantly and have allowed a wide variety of experimental conditions to be utilized.[41,42] Other examples have allowed such

(41) (a) Collman, J. P.; Cagne, R. R.; Reed, C. A.; Halbert, T. R.; Lang, G.; Robinson, W. T. *J. Am. Chem. Soc.* **1975**, *97*, 1427–1433. (b) Collman, J. P.; Brauman, J. I.; Halbert, T. R.; Suslick, K. S. *Proc. Natl. Acad. Sci. U.S.A.* **1976**, *73*, 3333–3337. (c) Collman, J. P. *Acc. Chem. Res.* **1977**, *10*, 265–272. (d) Collman, J. P.; Brauman, J. I.; Iverson, B. L.; Sessler, J. L.; Morris, R. M.; Bigson, Q. H. *J. Am. Chem. Soc.* **1983**, *105*, 3052–3064. (e) Collman, J. P.; Brauman, J. I.; Collins, T. J.; Iverson, B. L.; Lang, G.; Pettman, R. B.; Sessler, J. L.; Walters, M. A. *J. Am. Chem. Soc.* **1983**, *105*, 3038–3052 and references therein. (f) Almog, J.; Baldwin, J. E.; Dyer, R. L.; Peters, M. *J. Am. Chem. Soc.* **1975**, *97*, 226–227. (g) Budge, J. R.; Ellis, P. E., Jr.; Jones, R. D.; Linard, J. E.; Szymarski, T.; Basolo, F.; Baldwin, J. E.; Dyer, R. L. *J. Am. Chem. Soc.* **1979**, *1010*, 4762–4763.

(42) (a) Badger, G. M.; Jones, R. A.; Lazlett, R. L. *Aust. J. Chem.* **1964**, *17*, 1028–1035. (b) Groves, J. T.; Haushalter, R. C.; Nakamura, M.; Nemo, T. E.; Evans, B. J. *J. Am. Chem. Soc.* **1981**, *103*, 2884–2886. (c) Balch, A. L.; Chan, Y.-W.; Cheng, R.-J.; La Mar, G. N.; Latos-Grazynski, L.; Renner, M. W. *J. Am. Chem. Soc.* **1984**, *106*, 7779–7785. (d) Lee, W. A.; Calderwood, T. S.; Bruice, T. C. *Proc. Natl. Acad. Sci. U.S.A.* **1985**, *82*, 4301–4305.

factors as proximal imidazole strain to be explored.[23b,43] Thus, these synthetic porphyrin complexes have greatly contributed to our understanding of oxygen binding and activation.

However, the information that could be extrapolated to the proteins from the high-frequency RR spectra, as well as the optical absorption spectra of these artificial complexes, is limited.[44] This is the result of the altered pattern of peripheral substitution, which changes the normal modes[45] and the vibronic coupling[46] of the methine-substituted porphyrin complexes from that of the physiological type. On the other hand, for the β-pyrrole-substituted metalloporphyrins, the ν_{10} and ν_3 frequencies[47] show a well-quantified inverse correlation to the center to nitrogen distance, or core size, of the macrocycle and little dependence on the pyrrole C$_\beta$ substituents.[37] Thus, the high-frequency RR data from the protoporphyrin and octaethylporphyrin models are directly comparable to those for the protein adducts. Table II collects these and other structure-sensitive vibrational frequencies that we have measured for ferrous oxy and ferryl oxo octaethyl and protoporphyrin complexes and compares them to analogous data from the oxygenated protein species. The data in Table II for the LPO and MPO complexes come from the spectra reported in Figure 8 (see below). The table reveals that myeloperoxidase compounds II and III (MPO-II and MPO-III) exhibit lowered ν_s and ν_{10} frequencies and thus appear to have an expanded core size of ~2.00 Å, whereas ferryl oxo myoglobin (Mb=O) most likely has a contracted core size of ~1.98 Å[16b] compared to that of the models and the other protein adducts (~1.99 Å). The core size estimates predicted by the solution RR frequencies[37] are in excellent agreement with the EXAFS results.[48]

Other trends in the macrocycle vibrational frequencies of these ferrous oxy and ferryl oxo compounds are suggested by Table II. The ν_4 values of the (NMI)$_2$Fe^{III}, (NMI)Fe^{II}—O$_2$, and (NMI)-Fe^{IV}=O series exhibit a slight increase. In the models, octaethylporphyrin species have slightly higher ν_4 values than protoporphyrin complexes. In the proteins, the ν_4 value of ferryl oxo Mb is higher than that of HRP-II, while the ν_4 value of ferrous oxy Mb is lower than that of HRP-III. The lowered ν_4 values in the MPO relative to all other species are most likely due to structural differences in the heme macrocycle rather than differences in the iron center. The ν_2 frequencies for (NMI)Fe^{II}—O$_2$ porphyrins appear similar to those of the low-spin ferric (NMI)$_2$Fe^{III} compounds. However, for (NMI)Fe^{IV}=O adducts, this frequency is higher. Aside from MPO, lactoperoxidase (LPO) is the only protein represented in Table II that does not definitely contain a protoporphyrin IX prosthetic group. Thus, altered peripheral substituents may account for the lowered ν_2(C$_\beta$C$_\beta$) frequencies displayed by LPO-II and LPO-III relative to the others. All of these proteins are considered to be ligated proximally by histidine imidazole.[8]

RR spectra of LPO-II, LPO-III, MPO-II, and MPO-III appear in Figure 8. The LPO-II frequencies are in good agreement with those reported by Manthey et al.[49b] and Reczek et al.;[16c] however, the relative RR intensities differ owing to the different excitation wavelengths employed. As expected, the LPO-III high-frequency spectrum is very similar, consistent with an Fe^{II}—O$_2$ heme. The high-frequency spectrum of MPO-II at pH 7.0 is similar to that of the intermediate at pH 10.7.[20] Some differences in relative intensities, e.g., the feature at 1550 cm^{-1} being more intense at the lower pH, are apparent because of the different Soret absorption characteristics of the two forms.[50] Similar to that of LPO, the compound III spectrum of MPO is consistent with an Fe^{II}—O$_2$ configuration.

Discussion

One of the practical advantages of the RR technique over IR spectroscopy in the study of these compounds is that the iron–oxygen stretching frequencies of both ferryl oxo and ferrous oxy porphyrin model compounds and heme proteins can be measured. Other vibrations of interest, i.e. ν(O=O) and δ(FeOO), however, have not been accessed by the application of the RR technique to heme proteins. Although IR spectroscopy can be used to detect the ν(O=O) vibration in model compounds,[51] application of the technique to heme proteins is difficult.[52] This situation was partially overcome by substitution of Co^{II} for Fe^{II} in the dioxygen complex of heme proteins. Yu and co-workers[13a] demonstrated that ν(O=O) of cobaltous oxy heme proteins was strongly enhanced by RR excitation in the region of the Soret absorption. Related work in Nakamoto's lab demonstrated charge-transfer-enhanced RR detection of ν(O=O) in Co^{II}—O$_2$ complexes with a variety of equatorial ligands other than porphyrin.[53] These findings led to a large amount of RR work that has provided insight into the complex vibrational behavior of the ν(O=O) motion in six-coordinate cobaltous oxy porphyrin complexes both in vitro and in reconstituted proteins,[13,54,55] which is discussed, to some extent, below. In a similar regard, V^{IV}=O and Mn^{IV}=O complexes of porphyrins have recently been studied by Spiro's group as model systems for the Fe^{IV}=O compounds.[56] Although this work is important not only to heme proteins but also to enzymes that contain these metals, the extent to which these findings are quantitatively pertinent to in vivo heme iron centers remains to be established. With these considerations in mind, we

(43) (a) Young, R.; Chang, C. K. *J. Am. Chem. Soc.* **1985**, *107*, 898–909. (b) Traylor, T. G.; Chang, C. K.; Geibel, J.; Berzinis, A.; Mincey, T.; Cannon, J. *J. Am. Chem. Soc.* **1979**, *101*, 6716–6723. (c) Mitchell, M. L.; Campbell, D. H.; Traylor, T. G.; Spiro, T. G. *Inorg. Chem.* **1985**, *24*, 967–971.

(44) The chelated heme models prepared by Traylor's group are exceptions to this; however, RR spectra have been reported only for the ferrous–CO derivatives (see ref 43b,c).

(45) (a) Atamian, M.; Donohue, R. J.; Lindsey, J. S.; Bocian, D. F. *J. Phys. Chem.* **1989**, *93*, 2236–2243. (b) Li, X.-Y.; Czernuszewicz, R. S.; Spiro, T. G. *J. Am. Chem. Soc.*, in press.

(46) (a) Aramaki, S.; Hamaguchi, H.; Tasumi, M. *Chem. Phys. Lett.* **1983**, *96*, 555–559 (b) Kozuku, M. *J. Inorg. Biochem.* **1986**, *26*, 197–204.

(47) (a) Abe, M.; Kitagawa, T.; Kyogoku, Y. *J. Chem. Phys.* **1978**, *69*, 4526–4534. (b) Li, X.-Y.; Czernuszewicz, R. S.; Kincaid, J. R.; Stein, P.; Spiro, T. G. *J. Am. Chem. Soc.*, in press. (c) Choi, S.; Spiro, T. G.; Langry, K. C.; Smith, K. M.; Budd, D. L.; La Mar, G. N. *J. Am. Chem. Soc.* **1982**, *104*, 4345–4351.

(48) (a) Penner-Hahn, J. E.; McMurry, T. J.; Renner, M.; Latos-Grazynsky, L.; Eble, K. S.; Davis, I. M.; Balch, A. L.; Groves, J. T.; Dawson, J. H.; Hodgson, K. O. *J. Biol. Chem.* **1983**, *258*, 12761–12764. (b) Penner-Hahn, J. E.; Eble, K. S.; McMurry, T. J.; Renner, M.; Balch, A. L.; Groves, J. T.; Dawson, J. H.; Hodgson, K. O. *J. Am. Chem. Soc.* **1986**, *108*, 7819–7825. (c) Powers, L.; Sessler, J. L.; Woolery, G. L.; Chance, B. *Biochemistry* **1984**, *23*, 239–244. (d) Chance, M.; Powers, L.; Kumar, C.; Chance, B. *Biochemistry* **1986**, *25*, 1259–1265.

(49) (a) Andersson, L. A.; Renganathan, V.; Loehr, T. M.; Gold, M. H. *Biochemistry* **1987**, *26*, 2258–2263. (b) Manthey, J. A.; Boldt, N. J.; Bocian, D. F.; Chan, S. I. *J. Biol. Chem.* **1986**, *261*, 6734–6741.

(50) Hoogland, H.; Van Kuilenburg, A.; Van Riel, C.; Muijsers, A. O.; Wever, R. *Biochim. Biophys. Acta* **1987**, *916*, 76–82.

(51) (a) Nakamoto, K.; Watanabe, T.; Ama, T.; Urban, M. W. *J. Am. Chem. Soc.* **1982**, *104*, 3745–3746. (b) Watanabe, T.; Ama, T.; Nakamoto, K. *J. Phys. Chem.* **1984**, *88*, 440–445. (c) Kuroi, T.; Nakamoto, K. *J. Mol. Struct.* **1986**, *146*, 111–121.

(52) (a) Barlow, C. H.; Maxwell, J. C.; Wallace, W. J.; Caughey, W. S. *Biochem. Biophys. Res. Commun.* **1973**, *55*, 91–95. (b) Maxwell, J. C.; Volpe, J. A.; Barlow, C. H.; Caughey, W. S. *Biochem. Biophys. Res. Commun.* **1974**, *58*, 166–171. (c) Caughey, W. S.; Barlow, C. H.; Maxwell, J. C.; Volpe, J. A.; Wallace, W. J. *Ann. N.Y. Acad. Sci.* **1975**, *244*, 1. (d) Potter, W. T.; Tucker, M. P.; Houtchens, R. A.; Caughey, W. S. *Biochemistry* **1987**, *26*, 4699–4707.

(53) (a) Nakamoto, K.; Suzuki, M.; Ishiguro, T. Kozuka, M.; Nishida, Y.; Kida, S. *Inorg. Chem.* **1980**, *19*, 2822–2824. (b) Suzuki, M.; Ishiguro, T.; Kozuka, M.; Nakamoto, K. *Inorg. Chem.* **1981**, *20*, 1993–1996. (c) Nakamoto, K.; Nonaka, Y.; Ishiguro, T.; Urgan, M. W.; Suzuki, M.; Kozuka, Y.; Nishida, Y.; Kida, S. *J. Am. Chem. Soc.* **1982**, *104*, 3386–3391.

(54) (a) Bajdor, K.; Kincaid, J. R.; Nakamoto, K. *J. Am. Chem. Soc.* **1984**, *106*, 7741–7747. (b) Kincaid, J. R.; Proniewicz, L. M.; Bajdor, K.; Bruha, A.; Nakamoto, K. *J. Am. Chem. Soc.* **1985**, *107*, 6775–6781. (c) Proniewicz, L. M.; Nakamoto, K.; Kincaid, J. R. *J. Am. Chem. Soc.* **1988**, *110*, 4541–4545. (d) Bruha, A.; Kincaid, J. R. *J. Am. Chem. Soc.* **1988**, *110*, 6006–6014.

(55) (a) Mackin, H. C.; Tsubaki, M.; Yu, N.-T. *Biophys. J.* **1983**, *41*, 349–357. (b) Mackin Thompson, H. C.; Yu, N.-T.; Gersonde, K. *Biophys. J.* **1987**, *51*, 289–295.

(56) (a) Su, Y. O.; Czernuszewicz, R. S.; Miller, L. A.; Spiro, T. G. *J. Am. Chem. Soc.* **1988**, *110*, 4150–4157. (b) Czernuszewicz, R. S.; Su, O. Y.; Stern, M. K.; Macor, K. A.; Kim, D.; Groves, J. T.; Spiro, T. G. *J. Am. Chem. Soc.* **1988**, *110*, 4158–4165.

have used oxygen complexes with iron porphyrins rather than adducts of cobalt, vanadium, or other transition metals and have chosen porphyrin and proximal ligands to mimic the actual protein environment. Bond distance estimates from the Raman data[22b,26b,57] have been shown to correlate well with EXAFS measurements, particularly in the case of Fe^{IV}=O species,[16-21,26-30,48,58] and in the discussion below we use available vibrational data to identify those factors that allow the protein environment to fine tune the Fe-O bond to efficient function. We use the trends that emerge to interpret our recent RR measurements on ferryl oxo[19,20] and ferrous oxy[3] enzyme intermediates.

A. Factors Affecting the Iron-Oxygen Stretching Vibrations. In general, the factors affecting the iron-oxygen stretching frequency of ferrous oxy and ferryl oxo porphyrin models in solution are most likely the same as those influencing the CO and O_2 binding affinities (see ref 59 for recent reviews of iron-axial-ligand vibrations). These have been studied in detail[33,60] and include trans-ligand effects (which equate to proximal effects in the proteins), solvent or protecting group polarity (heme pocket polarity in the proteins), and steric and hydrogen-bonding interactions with the diatomic ligand (distal protein effects). The electron-donating capabilities of the substituents of the porphyrin ring exert a significant effect on the O_2 binding constant;[60a] however, this thermodynamic trend does not necessarily correlate with measurable changes in the iron-oxygen bond strength.[12,22] That is, the data presented in this paper and in our earlier work[31] show that the iron-oxygen stretching frequency of ferrous oxy and ferryl oxo hemes does not depend strongly on the electronic properties of the side chains of conventional model porphyrin complexes. Thus, the relationship between the binding affinity and the iron-ligand stretching frequency is not necessarily straightforward.[13,23] While the former parameter is more important to the understanding of oxygen transport by the globins, the trends in the iron-oxygen and oxygen-oxygen stretching frequencies are expected to be informative in understanding the process of oxygen activation (e.g., the splitting of the oxygen-oxygen bond in O_2 and H_2O_2 by oxidases and peroxidases, respectively). We focus first on $\nu(Fe^{IV}$=O) in model compounds and then on its behavior in ferryl oxo protein species. Next, we consider the $\nu(Fe^{II}$—$O_2)$ behavior in the models and, lastly, the protein influences on this vibration in ferrous oxy myoglobin, hemoglobin, peroxidase, and cytochrome oxidase.

B. Ferryl Oxo Species. In the Fe^{IV}=O structure, there is a strong σ interaction between the oxygen lone pair and the metal d_{z^2} orbital and a strong π overlap between the oxygen π^* and metal d_π (i.e. d_{xz} and d_{yz}) orbitals. In both of these interactions, electron donation is from the O^{2-} ligand to the Fe^{IV}.[26b,61]

Model Compounds. Table III clearly illustrates that a large trans-ligand effect influences the iron-oxygen vibration of the ferryl oxo species. In the absence of a strong ligand, in toluene, CH_2Cl_2, or THF solution, $\nu(Fe^{IV}$=O) occurs at 841-845 cm^{-1}. Introduction of NMI results in a 22-23-cm^{-1} decrease in this value. Thus, for this strong axial ligand six-coordinate complex, the $\nu(Fe^{IV}$=O) value is 818-820 cm^{-1} for all porphyrin complexes studied (with the exception of TpivPP, picket fence porphyrin, discussed below). Because the oxo ligand is both a strong σ donor and π donor, trans ligation by electron-donating ligands (e.g.

Table III. Iron–Oxygen Stretching Frequencies (cm^{-1}) of Ferryl Oxy Porphyrins and Heme Proteins[a]

model	$\nu(Fe^{IV}$=O)	solvent; temp	ref
Fe^{IV}=O(TPP)	852	Ar; −250 °C	26
Fe^{IV}=O(OEP)	852	Ar; −258 °C	26
Fe^{IV}=O(TMP)	843	toluene; −70 °C	29
Fe^{IV}=O(TMP)	845	toluene; −46 °C	40
Fe^{IV}=O(TMP)	841	CH_2Cl_2; −40 °C	28
(THF)Fe^{IV}=O(2,6-ClTPP)	841	THF; −50 °C	27b
(DMF)Fe^{IV}=O(2,6-ClTPP)	829	DMF; −50 °C	27b
(NMI)Fe^{IV}=O(2,6-ClTPP)	818	THF; −50 °C	27b
(NMI)Fe^{IV}=O(PPDME)	820	toluene; −120 °C	this work, 31
(NMI)Fe^{IV}=O(TPP)	820	toluene; −120 °C	this work, 31
(NMI)Fe^{IV}=O(OEP)	820	toluene; −120 °C	this work, 31
(THF)Fe^{IV}=O(T_{piv}PP)	829	THF; −50 °C	27a
(NMI)Fe^{IV}=O(T_{piv}PP)	807	THF; −50 °C	27a

protein	$\nu(Fe^{IV}$=O)	pH; temp	ref
Mb=O	797	pH 8.5; 20 °C	16b
HRP-II	775	pH 7; room temp	16a, 64
HRP-II	787	pH 11; room temp	17a, 63
MPO-II	782	pH 11; 5 °C	20
CCP-I	767, 753	pH 4–11; room temp	17b, 16c
LPO-II	745	pH 6–10; room temp	16c

[a] Abbreviations: TMP, tetramesitylporphyrin; TpivPP, tetrakis(o-pivalo-ylphenyl)porphyrin; Mb=O, ferryl oxo myoglobin; MPO-II, myeloperoxidase compound II; CcP-I, cytochrome c peroxidase compound I or ES; LPO-II, lactoperoxidase compound II.

imidazole) tends to lessen the donation from the oxo to the iron. As we and others noted earlier,[26b,27,31] this weakens the Fe^{IV}=O bond and decreases the stretching frequency.

Some effects of solvent on the value of $\nu(Fe^{IV}$=O) are apparent from Table III. Because we detect no change in $\nu(Fe^{IV}$=O) value over the −90 to −190 °C range, we attribute the ∼10-cm^{-1} decrease in the solution vs argon matrix values for the five-coordinate (or weakly ligated six-coordinate complexes) to the effects of solution rather than temperature. We further conclude that the effects of THF, CH_2Cl_2, and toluene upon the $\nu(Fe^{IV}$=O) value are very similar. We note that the values of $\nu(Fe^{IV}$=O) for the TpivPP complexes are 12–13 cm^{-1} below those of the other examples. In agreement with Su et al.,[56a] we attribute this to the polarizing effect of the pivalamido groups, which surround the oxo ligand. Thus, the observed decrease in $\nu(Fe^{IV}$=O) is more akin to a solvent effect rather than an electronic effect transmitted through the porphyrin macrocycle to the Fe center and caused by the difference in porphyrin substituents.

Prior to the present work, the most complete vibrational study of metalloporphyrin oxo complexes was reported by Su et al.,[56a] who used the more stable vanadyl (V^{IV}=O) porphyrins to model the ferryl oxo complexes. They established correlations between various environmental factors and the vanadium–oxygen stretching frequency, $\nu(V^{IV}$=O). Such detailed correlations are not yet possible for the ferryl oxo complexes, owing to the greater difficulty in the preparation and handling of the samples. Thus, consideration of the vanadyl work in the interpretation of the ferryl results is useful. For example, the trans-ligand effects on $\nu(Fe^{IV}$=O) appear similar but are smaller in magnitude than those manifest on $\nu(V^{IV}$=O). Solvent effects on the iron–oxo stretching frequency also appear qualitatively similar to those observed for the vanadium–oxo stretch; however, these are not yet quantitatively defined in the Fe^{IV}=O system. Thus, it is unclear to what extent the iron–oxo stretching frequency for the (DMF) Fe^{IV}=O(2,6-Cl_2TPP) complex reported by Gold et al.[27b] (see Table III) is influenced by trans-ligand vs solvent effects.

With regard to solvent effects, the analysis of the vanadyl oxo porphyrin spectra[56a] is useful in the interpretation of the ferryl oxo porphyrin results and provides a good interpretation of the ferryl-oxo stretching frequency of the picket fence porphyrin complex. However, not all of the trends in the metal–oxo stretching frequency observed in the vanadium compounds are recognized in the iron complexes discussed here. For example, the clear dependence of the metal–oxo stretching frequency upon

(57) Hershbach, D. R.; Laurie, V. W. *J. Chem. Phys.* **1961**, *35*, 458–463.
(58) Andersson, L. A.; Dawson, J. H. *Struct. Bonding*, in press.
(59) (a) Yu, N.-T. *Methods Enzymol.* **1986**, *130*, 351–409. (b) Yu, N.-T.; Kerr, E. A. in *Biological Applications of Raman Spectroscopy*; Spiro, T. G., Ed.; Wiley: New York, 1988; pp 39–95.
(60) (a) Traylor, T. G. *Acc. Chem. Res.* **1981**, *14*, 102–109. (b) Weschler, C. J.; Andersson, D. L.; Basolo, F. *J. Am. Chem. Soc.* **1975**, *97*, 6707–6713. (c) Collman, J. P.; Brauman, J. I.; Doxsee, K. M.; Sessler, J. L.; Morris, R. M.; Gibson, Q. H. *Inorg. Chem.* **1983**, *22*, 1427–1432. (d) Mispelter, J.; Momenteau, M.; Lavalette, D.; Lhoste, J. M. *J. Am. Chem. Soc.* **1983**, *105*, 5165–5167. (e) Suslick, K. S.; Fox, M. M.; Reinert, T. J. *J. Am. Chem. Soc.* **1984**, *106*, 4522–4525. (f) Traylor, T. G.; Koga, N.; Deardurff, L. A. *J. Am. Chem. Soc.* **1985**, *107*, 6504–6510. (g) Chang, C. K.; Ward, B.; Young, R.; Kondylis, M. P. *J. Macromol. Sci., Chem.* **1988**, *A25* (10&11), 1307–1326.
(61) Buchler, J. W.; Kokisch, W.; Smith, P. D. *Struct. Bonding* **1978**, *34*, 79–134.

Table IV. Iron–Histidine Stretching Frequencies (cm^{-1}) of Five-Coordinate Ferrous Porphyrins and Heme Proteins[a]

model	ν(Fe^{II}-Im)	ref
(2MI)Fe^{II}(T$_{piv}$PP)(CH$_2$Cl$_2$)	209	64a
(NMI)Fe^{II}(T$_{piv}$PP)(CH$_2$Cl$_2$)	225	52, 64a
(2MI)Fe^{II}(PPDME)(CH$_2$Cl$_2$)	200	47, 68a
(NMI)Fe^{II}(PPDME)(CH$_2$Cl$_2$)	~216	estimated from above values

protein	ν(Fe^{II}-His)	ref
Cyt Ox pH 7.4	214	67
Deoxy Mb (pH 7)	220	12b, 66
Deoxy Hb (pH 7)	215	12a, 65
HRP-C (alkaline)	241	68a
HRP-C (acidic)	244	68a
CcP (alkaline)	234	17b
CcP (acidic)	247	17b
MPO (pH 7.3)	248	62a
LPO (pH 8.5)	256	49b

[a] Abbreviations: Cyt Ox, cytochrome c oxidase; LPO, lactoperoxidase; 2MI, 2-methylimidazole; His, histidine imidazole; Im, generic imidazole species.

the nature of the porphyrin ring substituents in the five-coordinate vanadyl complexes[56a] is not detected in the six-coordinate ferryl complexes (see Table III).[31] This fact is significant to the interpretation of the ν(Fe^{IV}=O) frequencies obtained from the proteins. Because we detect no dependence of the ferryl–oxo stretching frequency upon the peripheral substituents of the porphyrins in these model compounds, we can focus on interpreting the ν(Fe^{IV}=O) frequencies in the enzyme intermediates in terms of protein effects along the z axis of the heme structure (see below). Thus, particularly for the ferryl oxo adducts, the vibrations of the Fe and axial ligands are orthogonal to and appear independent of the planar porphyrin vibrations. In particular, this has allowed us to analyze the iron–oxo stretching frequency of myeloperoxidase compound II (MPO-II; see Table III),[20] despite the perverse structure of the macrocycle.[62] We note, however, that oxidation of the porphyrin ring to a π cation radical, as in the compound I intermediates of peroxidases, may have a large effect on the ν(Fe^{IV}=O) frequency.[21,30,56a]

Proteins. Table III shows that the ν(Fe^{IV}=O) values for the protein species examined are all substantially lower than those of the model complexes. The environmental factors that can cause these lowered frequencies are the proximal trans-ligand strength, solvent effects (i.e. local protein pocket polarizability), and distal (e.g. hydrogen-bonding) influences. In particular, the trans–ligand strength of the proximal histidine most likely plays a key role. We would like to establish a spectroscopic parameter to quantify the trans-ligand effect on the iron–oxygen stretching frequency of these protein adducts. Ideally, we would like to compare the values of ν(Fe^{IV}—His) to those of ν(Fe^{IV}=O). Unfortunately the Fe^{IV}—His stretching frequency has not been identified in any ferryl protein species.[16–21,63] Furthermore, we were not able to detect this vibration in our Fe^{IV}=O model compound spectra. Similarly, Spiro's group noted the absence of the analogous vibration in the Raman spectra of six-coordinate (L)V^{IV}=O porphyrin complexes.[56a] They discussed the reasons for the lack of significant resonance enhancement of this mode in not only these but also in spectra of six-coordinate ferrous oxy hemes.[14a] On the other hand, in RR spectra of the five-coordinate (deoxy) ferrous heme proteins and model compounds, the ν(Fe^{II}-His) vibration is readily observed, and its relation to the O$_2$ binding affinity in the globins has been the subject of extensive study.[12,22b,64–66] As shown by
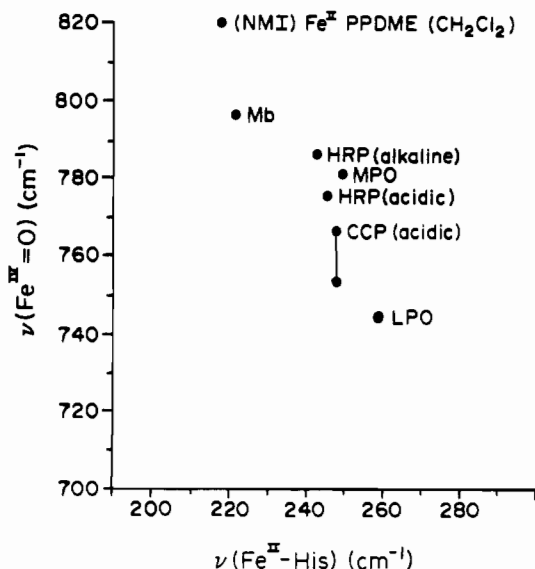

Figure 9. Plot of ν(Fe^{IV}=O) vs ν(Fe^{II}-His) demonstrating an inverse correlation between these two vibrational frequencies.

Table IV, these frequencies are consistently higher in the peroxidase species[68] than in the globins or the model compounds. Walters and Spiro[14a] and Van Wart and Zimmer[15] have made tentative assignments of the iron–histidine stretching frequencies in ferrous oxy Mb and HRP-III, and the frequency ordering of these modes in the two proteins agrees with the ν(Fe^{II}-His) values of the five-coordinate ferrous deoxy species. That is, for this example, the relative proximal ligand strengths of the heme moieties, as evidenced by the iron–histidine stretching frequencies, remains intact in these two different states (i.e., deoxy and ferrous oxy) of the proteins. That the stronger proximal histidine ligation in HRP compared to Mb is also present in the ferric states of the enzyme is implied by the shorter Fe–N(His) bond distance obtained from EXAFS measurements by Chance, Powers, and co-workers for HRP (~1.92 Å) compared to Mb (2.09 Å).[48c,d,69] It is generally thought that this stronger proximal trans ligation results in increased electron density at the iron, which in turn stabilizes the higher oxidation states of the heme and facilitates peroxidase activity.[58,69,70]

(62) (a) Babcock, G. T.; Ingle, R. T.; Oertling, W. A.; Davis, J. C.; Averill, B. A.; Hulse, C. L.; Stufkens, D. J.; Bolscher, B. G. J. M.; Wever, R. *Biochim. Biophys. Acta* **1985**, *828*, 58–66 and references therein. (b) Sibbett, S. S.; Hurst, J. K. *Biochemistry* **1984**, *23*, 3007–3013.
(63) (a) Sitter, A. J.; Reczek, C. M.; Terner, J. *J. Biol. Chem.* **1985**, *260*, 7515–7522. (b) Hashimoto, S.; Tatsuno, Y.; Kitagawa, T. *Proc. Natl. Acad. Sci. U.S.A.* **1986**, *83*, 2417–2421.
(64) (a) Hori, H.; Kitagawa, T. *J. Am. Chem. Soc.* **1980**, *102*, 3608–3613. (b) Stein, P.; Mitchell, M.; Spiro, T. G. *J. Am. Chem. Soc.* **1980**, *102*, 7795–7797. (c) Desbois, A.; Lutz, M.; Banerjee, R. *Biochim. Biophys. Acta* **1981**, *671*, 177–183.

(65) (a) Matsukawa, S.; Kawatari, K.; Yoneyama, Y.; Kitagawa, T. *J. Am. Chem. Soc.* **1985**, *107*, 1108–1113. (b) Kitagawa, T. In *Biological Applications of Raman Spectroscopy*; Spiro, T. G., Ed.; John Wiley & Sons: New York, 1988; pp 97–132.
(66) (a) Kitagawa, T.; Nagai, K.; Tsubaki, M. *FEBS Lett.* **1979**, *104*, 376–378. (b) Argade, P. V.; Sassaroli, M.; Rousseau, D. L.; Inubushi, T.; Ikeda-Saito, M.; Lapidot, A. *J. Am. Chem. Soc.* **1984**, *106*, 6593–6596. (c) Atamian, M.; Bocian, D. F. *Biochemistry* **1987**, *26*, 8319–8326. (d) Matsukawa, S.; Mawatari, K.; Yoneyama, Y.; Kitagawa, T. *J. Am. Chem. Soc.* **1985**, *107*, 1108–1113.
(67) (a) Salmeen, I.; Rimai, L.; Babcock, G. T. *Biochemistry* **1978**, *17*, 800–806. (b) Ogura, T.; Hon-nami, K.; Oshima, T.; Yoshikawa, S.; Kitagawa, T. *J. Am. Chem. Soc.* **1983**, *105*, 7781–7783.
(68) (a) Teraoka, J.; Kitagawa, T. *J. Biol. Chem.* **1981**, *256*, 3969–3977. (b) Desbois, A.; Mazza, G.; Stetzkowski, F.; Lutz, M. *Biochim. Biophys. Acta* **1984**, *785*, 161–176.
(69) (a) Powers, L.; Chance, B.; Ching, Y.; Angiolillo, P. *Biophys. J.* **1981**, *34*, 465–498. (b) Chance, B.; Powers, L.; Ching, Y.; Poulos, T. L.; Yamazaki, I.; Paul, K. G. *Arch. Biochim. Biophys.* **1984**, *235*, 596–611.
(70) (a) Schonbaum, G. R.; Houtchens, R. A.; Caughey, W. S. In *Biochemical and Clinical Aspects of Oxygen*; Caughey, W. S., Ed.; Academic Press: New York, 1979; pp 195–211. (b) Schonbaum, G. R.; Lo, S. *J. Biol. Chem.* **1972**, *247*, 3353. (c) Peisach, J. *Ann. N.Y. Acad. Sci.* **1975**, *244*, 187. (d) Mincey, T.; Traylor, T. G. *J. Am. Chem. Soc.* **1979**, *101*, 765. (e) Poulos, T. L.; Kraut, J. *J. Biol. Chem.* **1980**, *255*, 8199–8205. (f) Poulos, T. L.; Freer, S. T.; Alben, R. A.; Edwards, S. L.; Skogland, U.; Tako, K.; Erikson, B.; Xuong, N.; Yonetoni, T.; Kraut, J. *J. Biol. Chem.* **1980**, *255*, 575–580. (g) Finzel, B. C.; Poulos, T. L.; Kraut, J. *J. Biol. Chem.* **1984**, *259*, 13027–13036. (h) Yuan, L.-C.; Bruice, T. C. *J. Am. Chem. Soc.* **1986**, *108*, 1643–1650. (i) Traylor, T. G.; Popovitz-Biro, R. *J. Am. Chem. Soc.* **1988**, *110*, 239–243. (j) Thanabal, V.; de Ropp, J. S.; La Mar, G. N. *J. Am. Chem. Soc.* **1988**, *110*, 3027–3035. (k) Shiro, Y.; Takida, M.; Morishima, I. *J. Am. Chem. Soc.* **1988**, *110*, 4030–4035.

Table V. Iron–Oxygen and Oxygen–Oxygen Stretching Frequencies (cm^{-1}) of Ferrous Oxy Porphyrins and Heme Proteins

model	$\nu(Fe^{II}-O_2)$	solvent; temp	$\nu(O=O)$	solvent; temp	ref
Fe^{II}—O$_2$(TPP)	509	O$_2$; –248 °C	1195	O$_2$, –248 °C	24a
(NMI)Fe^{II}—O$_2$(OEP)	573	DMF; –120 °C			this work
	572	CH$_2$Cl$_2$; –120 °C			this work
(NMI)Fe^{II}—O$_2$(PP)	573	CH$_2$Cl$_2$; –120 °C			this work
(NMI)Fe^{II}—O$_2$(PA)	576	CH$_2$Cl$_2$; –120 °C			this work
(1,2MI)Fe^{II}—O$_2$(T$_{piv}$PP)	562	benzene; room temp			23a
	564	CH$_2$Cl$_2$; room temp			22b
	567	CH$_2$Cl$_2$; –40 °C			22b
	558	solid; room temp			22b
(NMI)Fe^{II}—O$_2$(T$_{piv}$PP)	571	benzene; room temp			23a
	568	CH$_2$Cl$_2$; room temp			22
	570	CH$_2$Cl$_2$; –40 °C			22b
	567	solid; room temp			22b
			1159	nujol, room temp	41b
(NMI)Fe^{II}—O$_2$[(Piv)$_2$C$_n$)]	563	benzene; room temp			25
(PIP)Fe^{II}—O$_2$(TPP)	575	toluene; ~70 °C			24
			1157	CH$_2$Cl$_2$, –68 °C	24b
(PIP)Fe^{II}—O$_2$(TMP)	568	toluene; –78 °C			40

protein	$\nu(Fe^{II}-O_2)$	pH; temp	ref
Hb—O$_2$	571	pH 8.5; 10 °C	12a, 13, 14
Mb—O$_2$	572	pH 7.2; 10 °C	12b
Mb—O$_2$	569	pH 6.8; –15 °C	15
HRP-III	559	pH 6.8; –15 °C	15
Cyt Ox a_3—O$_2$	571	pH 7.4; 10 °C	3

Thus, we estimate the relative trans-ligand strengths by comparison of the reported Fe^{II}—His frequencies for the five-coordinate ferrous species. Figure 9 demonstrates the apparent linear correlation of $\nu(Fe^{IV}=O)$ to $\nu(Fe^{II}$—His) This suggests that the trans-ligand effect is the major determinant of the iron–oxo stretching frequency in the proteins and that, in the first approximation, similar protein interactions are operative on the proximal histidine in these different oxidation states. This modification of the trans-ligand strength is most likely attributed to hydrogen bonding of the 1-proton on the histidyl imidazole group to a proximal amino acid group of the protein.[68-70] The resulting stronger trans-ligand bond further weakens the Fe$^{IV}=O$ bond, which is already weak relative to other transition-metal–oxo bonds,[71] and presumably increases its chemical activity. These trans-ligand effects in oxygen-metabolizing problems provide an excellent example of protein-induced modification of the properties of bound catalytic intermediates. This process is likely to be of much greater importance in peroxidases than in the globins.[72]

Hydrogen bonding of the oxo ligand of horseradish peroxidase compound II (HRP-II) to a protonated distal histidine residue has been suggested to explain the pH dependence of the iron–oxygen stretching frequency measured by RR spectra.[63] Indeed, the variation of the $\nu(Fe^{IV}=O)$ frequency corresponds to pH-dependent trends in the kinetic rate constants.[8b] The pH at which these spectral and kinetic changes occur clearly reflects the pK_a of a distal protein residue, and hydrogen bonding of the oxo ligand to this ionizable proton at pH values below this pK_a is consistent with the catalytic mechanism proposed for this enzyme.[8] Accordingly, the 12-cm^{-1} decrease in the $\nu(Fe^{IV}=O)$ frequency of HRP-II upon lowering the pH from 11 to 7 (Table III) has been

attributed to the effects of distal hydrogen bonding. However, because ionization of the distal protein residue may be linked to changes in hydrogen bonding of the proximal histidine gland, as was suggested for the ferrous enzyme,[68a] the strength of the trans-ligand bond may also be pH-dependent. This is the case for ferrous HRP as the $\nu(Fe^{II}$—His) varies with pH between 241 and 244 cm^{-1} (see Table IV).[68a] Thus, the 12-cm^{-1} difference in the $\nu(Fe^{IV}=O)$ frequencies of HRP-II may be caused by either the *distal* hydrogen bonding of the oxo group at the lower pH or the possible increase in trans-ligand strength or a combination of both effects. Although further systematic vibrational studies will be necessary to establish rigorously the relative importance of these two distinct protein environmental effects on $\nu(Fe^{IV}=O)$, our analysis suggests that the major determinant of this vibrational frequency is the trans-ligand strength of the proximal histidine.

C. Ferrous Oxy Species. In six-coordinate hemes, O$_2$ binds to ferrous iron in a bent, end-on configuration.[73] Electrons are donated from one of the dioxygen π^* orbitals to the metal d$_{z^2}$ orbital via a σ interaction. In contrast, π electrons from the Fe(d$_{xz}$) orbital are accepted by the other π^* orbital of the oxy ligand.[59,74] The π-acceptor properties of the dioxygen are thought to be stronger than the σ-donor properties.[23a] This "push-pull" bonding situation may account for the opposite trend that the $\nu(Fe^{II}$—O$_2$) and $\nu(Fe^{IV}=O)$ frequencies of the model compounds display as a function of trans-ligand strength. This point is considered in more detail below.

Model Compounds. Table V collects $\nu(Fe^{II}$–O$_2$) frequencies for the model compounds studied here as well as for several other models and a number of heme proteins. The recent work of Wagner et al.,[24a] presented in Table V, reveals that a large increase in the $\nu(Fe^{II}$–O$_2$) frequency, approximately 66 cm^{-1}, occurs upon introduction of a strong trans-ligand such as piperidine (PIP) to the five-coordinate ferrous oxy TPP complex. From the table it is also evident that substitution of PIP for NMI does not change $\nu(Fe^{II}$–O$_2$) greatly. On the other hand, the work of Walters et

(71) Mayer, J. M. *Inorg. Chem.* **1988**, *27*, 3899–3903.
(72) Ondrias, M. R.; Rousseau, D. L.; Shelnutt, J. A.; Simon, S. R. *Biochemistry* **1982**, *21*, 3428–3437. We note that the technique of approximating the proportional trans-ligand strength in the six-coordinate iron heme proteins by the $\nu(Fe^{II}$–His) of the five-coordinate (deoxy) complex can not be used for comparing the R and T states of ferrous carbonyl hemoglobin (Gersonde, K.; Kerr, E.; Yu, N.-T.; Parish, D. W.; Smith, K. M. *J. Biol. Chem.* **1986**, *261*, 8678–8685.). Furthermore, despite differences of ~6 cm^{-1} in the $\nu(Fe^{II}$–His) of the R and T states of deoxy Hb, the $\nu(Fe^{II}$–O$_2$) frequencies of ferrous–oxy R and T forms show no interpretable trend.[12] This shows that the R and T states of Hb represent a special case of heme–apoportein interaction. Hence, no attempt to include these states of Hb in Figure 9 was made. What we have done in Figure 9 rather is to compare the iron–oxygen stretching frequencies of a series of heme proteins that display a *wide* range of proximal histidine ligand strengths as evidenced by not only a ~40 cm^{-1} spread in their five-coordinate $\nu(Fe^{II}$–His) frequenices but also a plethora of other studies.[70]

(73) (a) Pauling, L.; Coryell, C. D. *Proc. Natl. Acad. Sci. U.S.A.* **1936**, *22*, 210–217. (b) Pauling, L. *Nature* **1964**, *203*, 182–183. (c) Collman, J. P.; Gagne, R. R.; Reed, C. A.; Robinson, W. T.; Rodley, G. A. *Proc. Natl. Acad. Sci. U.S.A.* **1974**, *71*, 1326–1329. (d) Jameson, G. B.; Rodley, G. A.; Robinson, W. T.; Gagne, R. R.; Reed, C. A.; Collman, J. P. *Inorg. Chem.* **1978**, *17*, 850–857. (e) Jameson, G. B.; Molinaro, F. S.; Ibers, J. A.; Collman, J. P.; Brauman, J. I.; Rose, E.; Suslick, K. S. *J. Am. Chem. Soc.* **1980**, *102*, 3224. (f) Phillips, S. E. V. *J. Mol. Biol.* **1980**, *142*, 531–554. (g) Shaanan, B. *Nature* **1982**, *296*, 683–684.
(74) (a) Reed, C. A. in *Metal Ions in Biological Systems*; Sigel, H., Ed.; Marcel Dekker: New York, 1978; Vol. 7, pp 277–310. (b) Gubelmann, M. H.; Williams, A. F. *Struct. Bonding* **1983**, *55*, 1–65.

Table VI. Factors Affecting Iron–Oxygen Stretching Frequencies (cm^{-1}) in Heme Model Compounds

factor	trend in Fe–O stretching frequency	
	$\nu(Fe^{II}$—O$_2)$	$\nu(Fe^{IV}$=O$)$
1. increase in trans-ligand strength	increase	decrease
2. increase in solvent acceptor number	?	decrease
3. variation in electronic effects of porphyrin substituents	negligible change	negligible change
4. decrease in temperature	slight increase	negligible change
5. conversion from solution to solid state	slight decrease	?
6. steric or hydrogen-bonding interaction with oxygen ligand	decrease with increasing α(FeOO) angle[a]	?

[a] The effects on $\nu(Fe^{II}$—O$_2)$ of hydrogen bonding *without* geometric distortion have not yet been determined.

al.[22b] and Kerr et al.[23a] collected in Table V clearly demonstrates a 3–9-cm^{-1} increase in the iron–oxygen stretching frequency upon substitution of NMI for 1,2-dimethylimidazole (1,2MI) as the sixth ligand of the ferrous oxy complex. The steric effects of the 2-methyl group weaken the iron–imidazole bond, as evidenced by the $\nu(Fe^{I}$I–Im) frequency of the five-coordinate ferrous complexes (see Table IV). Thus, the work of Nakamoto's, Spiro's, and Yu's groups indicates that the $\nu(Fe^{II}$—O$_2)$ frequency increases as the strength of the trans ligand increases, which suggests that the increased donation by the trans ligand into the Fe^{II}(d$_x$) orbitals enhances the strength of the Fe^{II}–O$_2$ bond, consistent with the arguments given above concerning the relative strengths of the σ and π bonding in the ferrous oxy complex.

The direct dependence of $\nu(Fe^{II}$—O$_2)$ on trans-ligand strength contrasts with the inverse dependence discussed above of ν-(Fe^{IV}=O) on axial ligation. This is noted in Table VI where we summarize the effects of various environmental parameters on the iron–oxygen stretching frequency of Fe^{II}—O$_2$ model compounds and compare them to the effects on the analogous Fe^{IV}=O vibration. For ferrous oxy complexes of picket fence porphyrin, the $\nu(Fe^{II}$—O$_2)$ vibrational frequency increases with lowered temperature and appears to decrease in solid compared to solution samples. Furthermore, little interpretable change in the ν-(Fe^{II}—O$_2)$ frequency of the unprotected OEP complex can be detected in DMF vs CH$_2$Cl$_2$ solvent (see Table V). These trends are all in contrast to those of the ferryl oxo complexes. On the other hand, similar to that of the Fe^{IV}=O samples,[31] the iron–oxygen stretching frequency of the Fe^{II}—O$_2$ model compounds shows little variation due to the electronic effects of different porphyrin pyrrole substituents. The latter observation is in agreement with earlier findings of Kitagawa and co-workers.[12b]

As noted in Table VI, the effects on the iron–oxygen stretching frequency of steric or hydrogen-bonding interaction with the oxygen ligand has not yet been established for ferryl oxo model compounds. Recently, however, a ferrous oxy porphyrin complex, (NMI)Fe^{II}—O$_2$[(Piv)$_2$C$_n$], which is thought to exhibit distal hydrogen bonding resulting in geometric distortion of the Fe^{II}—O=O bonding, has been investigated via RR measurements.[25] The $\nu(Fe^{II}$—O$_2)$ value (563 cm^{-1}, Table V) is 8 cm^{-1} lower than that for the picket fence porphyrin complex (NMI)Fe^{II}—O$_2$-(TpivPP) under the same conditions. The former porphyrin possesses both a polymethylene handle and a pair of pivalamido pickets. It has been suggested that weak hydrogen bonding could occur between the dioxygen ligand and the NH atoms of the amide linkages in the protecting groups of ferrous oxy picket fence porphyrin. However, as discussed by Chang et al.,[60g] because of the relatively large distance involved (4 Å), this interaction is more likely to be of a nonbonding, dipole–dipole nature. From Table V, we note that the $\nu(Fe^{II}$—O$_2)$ value measured for (NMI)-Fe^{II}-O$_2$(TpivPP) in CH$_2$Cl$_2$ at –40 °C approaches the frequency that we measured for the analogous OEP complex, indicating that the pivaloyl groups do not influence the $\nu(Fe^{II}$—O$_2)$ frequency as strongly as they do the $\nu(Fe^{IV}$=O) frequency (see Table III, above). This further suggests that the latter vibrational frequency is more sensitive to dipole interactions (hence solvent effects) than the $\nu(Fe^{II}$—O$_2)$ frequency, consistent with the observations listed in Table VI. This interpretation is consistent with the work of Mispeller et al.[60d] and Desbois et al.,[25] as they conclude that the hydrogen bonding exhibited by their ferrous oxy model occurs at the NH groups of the polymethylene handle, rather than at the

pivalamido moieties. This interaction accounts for the 8-cm^{-1} lowering of the $\nu(Fe$–O$_2)$ frequency of the [(Piv)$_2$C$_n$] complex compared to TpivPP complex and is discussed in more detail below.

Similar to the bis(picket fence)(handle)porphyrin of Momenteau and co-workers,[25,60d] the ferrous oxy complex of tetramesitylporphyrin (TMP) appears to exhibit a lower $\nu(Fe^{II}$—O$_2)$ frequency than the analogous TPP complex. This is illustrated by the entries of Table V for the piperidine-ligated complexes. The $\nu(Fe^{II}$—O$_2)$ frequency of (PIP)Fe^{II}–O$_2$(TPP) is 575 cm^{-1}, whereas it is lowered to 568 cm^{-1} for (PIP)Fe^{II}–O$_2$(TMP) under similar conditions. With the exception of the iron–oxygen stretching frequency of 509 cm^{-1} for the five-coordinate complex of Wagner et al.,[24a] these 7–8-cm^{-1} decreases in $\nu(Fe^{II}$–O$_2)$ for the [(Piv)$_2$C$_n$] and TMP complexes are the most dramatic observed to date for heme model compounds.

Thus far, our discussion has treated the $\nu(Fe^{II}$—O$_2)$ mode in the same manner as the $\nu(Fe^{IV}$=O) mode. The situation is more complex, however, as other vibrational motions, not only the $\nu(Fe^{II}$—His) mode but also the $\nu(O$=O) and the $\delta(FeOO)$ modes, are now involved. The RR-active, oxygen isotope sensitive vibration of ferrous oxy porphyrins at ~570 cm^{-1} is probably not a pure $\nu(Fe^{II}$—O$_2)$ motion but, rather, is likely to have some contribution from the $\delta(FeOO)$ internal coordinate.[75] The degree of mixing of the two coordinates in the observed mode is a function of both the α(FeOO) angle and the force constant of the Fe—O bond. The normal-coordinate analysis of the Fe^{II}—O=O group by Bajdor et al.[39] shows that for the range of α values displayed by the ferrous oxy models and Mb—O$_2$ (130–160°),[73] and at physically reasonable values of the Fe-O force constant (>1.90 mdyn/Å), the predominant internal coordinate of the ~570-cm^{-1} mode is $\nu(Fe^{II}$—O$_2)$ rather than $\delta(FeOO)$. X-ray crystal structures of (2MI)Fe^{II}–O$_2$(TpivPP)[73e] and (NMI)Fe^{II}–O$_2$(TpivPP)[73c,d] reveal α(FeOO) angles of $\sim130°$ for both complexes. The Fe–O and Fe–N(imidazole) distances are larger, however, by 0.15 and 0.04 Å, respectively, for the 2MI complex. As pointed out by Walters et al.,[22b] the 11-cm^{-1} decrease in $\nu(Fe^{II}$-O$_2)$ in the hindered 2MI complex is much less than predicted by Badger's rule. Thus, there must be changes in the Fe–O force constant that partially compensate for the difference in the Fe–O distance.

The effects of distal interactions, such as hydrogen-bonding, on $\nu(Fe^{II}$—O$_2)$ are likely to be distinct from those manifest on $\nu(Fe^{IV}$=O). This is the result of the increased size of the ligand and the preferably bent orientation of the dioxygen ligand in ferrous oxy compounds, relative to the simpler and more compact axial ligand situation in the ferryl oxo complexes. In order to discuss these effects in Fe^{II}—O$_2$ hemes, we must first explore the relationship between the metal–oxygen and oxygen–oxygen stretching frequencies in dioxygen complexes.

Yu and co-workers have proposed an inverse relationship between the $\nu(Co^{II}$—O$_2)$ and $\nu(O$=O) frequencies in cobaltous oxy hemes.[55,59] Prior to that, Nakamoto et al.[53c] quantitatively demonstrated a reciprocal square relationship between the cobalt-oxygen and oxygen–oxygen stretching frequencies of (L)Co^{II}—O$_2$—Co^{II}(L) compounds. For cobaltous oxy porphyrins the most dramatic illustration of this inverse trend comes from comparison of the $\nu(Co^{II}$—O$_2)$ and $\nu(O$=O) frequencies at 345 and 1278 cm^{-1},

(75) Benko, B.; Yu, N.-T. *Proc. Natl. Acad. Sci. U.S.A.* **1983**, *80*, 7042–7046.

respectively, for the five-coordinate Co^{II}—$O_2(TPP)^{76c}$ to those of the six-coordinate complexes, which display frequencies of ~ 510–530 and ~ 1135–1160 cm^{-1}, respectively.[54,55,76,77] Furthermore, these frequencies for TpivPP complexes with 1,2MI and NMI as sixth ligands,[54a,55a] as well for the (PIP) Co^{II}–O_2 (TPP) complexes in CH_2Cl_2 vs $C_6H_5CH_3$ solvents,[76c] are consistent with this trend. However, interpretation of the $\nu(O{=}O)$ frequency of both six-coordinate cobaltous and ferrous oxy porphyrins is complicated by vibrational coupling.[13,52,54,55] These interactions can change $\nu(O{=}O)$ values without affecting $\nu(Co^{II}$—$O_2)^{78}$ and, thus, could possibly obscure this trend for small perturbations of the $\nu(Co^{II}$—$O_2)$ frequency. Kincaid and co-workers[54,78] have recently provided a detailed interpretation of this phenomenon and find that the $\nu(O{=}O)$ motion can couple with vibrations of both the solvent and the trans ligand in the model compounds and with both proximal and distal amino acid residues in the reconstituted globins.[54] Until these effects of vibrational coupling are quantitatively defined, however, the exact (i.e., intrinsic or unperturbed) $\nu(O{=}O)$ frequencies, particularly in ferrous oxy proteins,[13,52] will remain controversial.

Reinspection of Table V, with attention to the $\nu(O{=}O)$ as well as the $\nu(Fe^{II}$—$O_2)$ frequencies of the five-coordinate Fe^{II}—$O_2(TPP)$ complex compared to those of $(NMI)Fe^{II}$—$O_2(TpivPP)$ and $(PIP)Fe^{II}$—$O_2(TPP)$, suggests an inverse trend between the metal–oxygen and oxygen–oxygen stretching frequencies, analogous to that of the cobalt system. Indeed, inclusion of the 488- and 1207-cm^{-1} values, respectively, obtained for the phthalocyanate complex, Fe^{II}—$O_2(PC)$,[39] further suggests an apparent inverse linear correlation between the $\nu(Fe^{II}$—$O_2)$ and $\nu(O{=}O)$ frequencies of the model compounds. Because these examples span a wide range of frequencies, the effects of vibrational coupling of the $\nu(O{=}O)$ are not significant.

The normal coordinate analysis of the Fe^{II}—O_2 vibrations by Bajdor et al.[39] and Desbois et al.[25] are consistent with this proposed inverse trend. The latter calculations illustrate the dependencies of the $\nu(Fe^{II}$—$O_2)$ and $\nu(O{=}O)$ frequencies on the $\alpha(FeOO)$ angle. Because the decrease in $\nu(Fe^{II}$—$O_2)$ in their model seemed contrary to the slight increase in $\nu(Co^{II}$—$O_2)$ observed by Odo et al.[17] upon hydrogen bonding of the oxy ligand in $(L)Co^{II}$—$O_2(TneoPP)$, Desbois et al.[25] reasoned that the $\alpha(FeOO)$ angle is increased in $(NMI)Fe^{II}$—$O_2[(Piv)_2C_n]$ compared to the TpivPP analogue as a result of the hydrogen bond. This is an attractive suggestion, as it could also explain the low $\nu(Fe^{II}$—$O_2)$ frequency of $(PIP)Fe^{II}$—$O_2(TMP)$ (see Table V). That is, the mesityl methyl groups could produce a similar geometric distortion in this compound. The crystal structures and $\nu(O{=}O)$ frequencies of these ferrous oxy compounds would test this hypothesis.

Proteins. Above, we found the major environmental determinant of the iron–oxygen stretching frequency of ferryl oxo hemes to be the trans-ligand interaction. We noted an inverse correlation between this $Fe^{IV}{=}O$ stretching frequency and the $\nu(Fe^{II}$—$Im)$ frequency for the models and the $\nu(Fe^{II}$—$His)$ frequency for the proteins. On the other hand, for the model compounds, a direct correlation seems likely between $\nu(Fe^{II}$—$O_2)$ and $\nu(Fe^{II}$—$Im)$, as exemplified by the values for the picket fence porphyrin (TpivPP) complexes in CH_2Cl_2 at room temperature (see Tables IV and V). This is consistent with the π-acceptor properties of the dioxygen ligand: increased π donation from imidazole will enhance the $Fe(d_\pi)$ donation to the $O_2(\pi^*)$ orbital and tend to strengthen the Fe–O bond. However, the $\nu(Fe^{II}$-$O_2)$ and $\nu(Fe^{II}$–$His)$ values obtained from Tables V and IV, respectively, for the *proteins* are contrary to this trend. That is, the peroxidase appears to exhibit

an inverse correlation of $\nu(Fe^{II}$-$O_2)$ to $\nu(Fe^{II}$–$His)$, whereas the Cyt Ox a_3–O_2 intermediate displays a typical iron-oxygen stretching frequency despite its fairly low $\nu(Fe^{II}$–$His)$.

Why do the ferrous oxy protein species appear to display a different trans-ligand effect than the ferrous oxy model compounds? It is possible that in the proteins the π donor interactions of O_2 become more important than the π acceptor properties in determining the trends in $\nu(Fe^{II}$-$O_2)$ as a function of the trans ligand. In order to explain the HRP-III result, Van Wart and Zimmer[15] proposed that the stronger proximal histidine ligation of the peroxidase with respect to the globin results in a reduction of the σ bonding that overrides an increase in π bonding between iron and dioxygen.

An alternative explanation can be developed from the arguments presented here. We suggest that in the proteins the proximal trans-ligand effect on $\nu(Fe^{II}$-$O_2)$ is actually similar to that of the models but is obscured by distal interactions of the dioxygen and the protein that act to produce an opposite trend. The larger size of dioxygen makes a distal interaction with the protein more likely in ferrous oxy adducts than in ferryl oxo species. Thus, we assert that in general the Fe–O bond in ferryl oxo heme proteins is influenced primarily by the proximal environment, whereas the Fe–O bond strength and hence $\nu(Fe^{II}$-$O_2)$ in the ferrous oxy species is modulated by the distal protein environment. Hydrogen bonding between the distal O atom of the dioxygen ligand and a protein residue is expected in both globins[73a,b,79–83] and ferrous oxy peroxidase[70j,84] and could feasibly alter the $\nu(Fe^{II}$-$O_2)$ value. Similar interactions were proposed to lower the $\nu(Fe^{IV}{=}O)$ value in HRP-II below pH 9.[63] The iron–oxygen stretching frequency of the ferrous oxy heme is likely to be less sensitive than that of the ferryl oxo complex, however, since the perturbation is one atom removed. By this reasoning, the $\nu(O{=}O)$ value of the Fe^{II}-O_2 moiety may be more sensitive to hydrogen-bonding than the ν-$(Fe^{II}$—$O_2)$ value.

RR measurements on $(Pyr)Co^{II}$—$O_2(TPP)$ in CH_2Cl_2 revealed only a small 3–5-cm^{-1} decrease in $\nu(O{=}O)$ upon addition of 20% methanol; this was interpreted to reflect the effects of weak hydrogen-bonding of the oxy ligand.[54a] The $\nu(Co$—$O_2)$ value was not reported. A more recent study of cobaltous oxy complexes of atropisomers of picket fence porphyrins reveals that stronger hydrogen bonding of the dioxygen ligand can lower the $\nu(O{=}O)$ by 10 cm^{-1} and possibly *raise* the $\nu(Co$—$O_2)$ frequency by 4 cm^{-1}.[77] X-ray crystal structures of oxyhemoglobin[82] and neutron diffraction studies of oxymyoglobin[81] reveal that the oxy ligand is hydrogen bonded to the distal histidine in the α subunits of Hb and in Mb but not in the β-Hb subunits. Measurements of O_2 and CO binding affinities on various mutants lacking the distal histidine are consistent with these findings.[83] RR measurements of Fe/Co hybrids of intact oxy Hb and isolated α—Co—O_2 and β—Co—O_2 subunits suggest that there is little difference in the $\nu(O{=}O)$ values of the oxy cobalt chromophore in the α- and β-subunits of Hb and of Mb.[13,85] Thus, if indeed the α-subunits exhibit hydrogen bonding that is absent in the β-subunits in solution, we must conclude that the effects of such hydrogen bonding are not obvious in the $\nu(O{=}O)$ and presumably the $\nu(Co$—$O_2)$ frequencies. We further suggest that these conclusions hold for the analogous vibrations of the ferrous oxy proteins, and that the

(76) (a) Jones, R. D.; Budge, J. R.; Ellis, Jr., P. E.; Linard, J. E.; Summerville, D. A.; Basolo, F. *J. Organomet. Chem.* **1979**, *181*, 151–158. (b) Jones, R. D.; Summerville, D. A.; Basolo, F. *Chem. Rev.* **1979**, *79*, 139–179. (c) Kozuka, M.; Nakamoto, K. *J. Am. Chem. Soc.* **1981**, *103*, 2162–2168. (d) Bajdor, K.; Nakamoto, K.; Kincaid, J. *J. Am. Chem. Soc.* **1983**, *105*, 679–681. (e) Nakamoto, K.; Paeng, I. R.; Kuroi, T.; Isobe, T.; Oshio, H. *J. Mol. Struct.* **1988**, *189*, 293–300.

(77) Odo, J.; Imai, H.; Kyuno, E.; Nakamoto, K. *J. Am. Chem. Soc.* **1988**, *110*, 742–748.

(78) Proniewicz, L. M.; Kincaid, J. R. *J. Am. Chem. Soc.* **1990**, *112*, 675–681.

(79) Perutz, M. F. In *Molecular Basis of Blood Diseases*; Stammatoyanopoulos, et al., Eds.; Saunders: Philadelphia, PA, 1987; pp 127–178.

(80) (a) Yonetoni, T.; Yamamoto, H.; Izuka, T. *J. Biol. Chem.* **1974**, *249*, 2168–2174. (b) Ikeda-Saito, M.; Hori, H.; Inbushi, T.; Yonetoni, T. *J. Biol. Chem.* **1981**, *256*, 10267–10271. (c) Walker, F. A.; Bowen, J. *J. Am. Chem. Soc.* **1985**, *107*, 7632–7635. (d) Lecomte, J. T. J.; La Mar, G. N. *J. Am. Chem. Soc.* **1987**, *109*, 7220–7222.

(81) Phillips, S. E. V.; Schoenborn, B. P. *Nature* **1981**, *292*, 81–82.

(82) Shaanan, B. *J. Mol. Biol.* **1983**, *171*, 31–59.

(83) Olson, J. S.; Mathews, A. J.; Rohlfs, R. J.; Springer, B. A.; Egeberg, K. D.; Sligar, S. G.; Tame, J.; Renaud, J.-P.; Nagai, K. *Nature*, in press.

(84) Yamada, H.; Yamazaki, I. *Arch. Biochem. Biophys.* **1975**, *171*, 737–744.

(85) (a) Kitagawa, T.; Ondrias, M. R.; Rousseau, D. L.; Ikeda-Saito M.; Yonetoni, T. *Nature* **1982**, *298*, 869–871. (b) Kaminaka, S.; Ogura, T.; Kitagishi, K.; Yonetoni, T.; Kitagawa, T. *J. Am. Chem. Soc.* **1989**, *111*, 3787–3794.

altered $\nu(Fe^{II}-O_2)$ value reported for HRP-III may be attributable to some other type of distal perturbation.

For insight into the nature of this perturbation, we consider the function, in particular the initial reaction steps, of a peroxidase. The peroxidase heme pocket binds hydrogen peroxide in a manner that facilitates the cleavage of the O—O bond. This is most likely accomplished by the action of a positively charged arginine group that pulls electron density out of the O—O bond of the peroxide.[70e] Removal of electron density from the O=O bond of dioxygen, however, *strengthens* the bond because the HOMO is antibonding. Thus, when O_2 rather than HOOH is bound in the peroxide heme crevice, the oxygen–oxygen bond is strengthened and $\nu(O=O)$ increases while $\nu(Fe^{II}-O_2)$ decreases. These distal effects on the electron density in the O=O bond of the bound dioxygen presumably overshadow the trans-ligand effects of the proximal histidine and thus explain the $\nu(Fe^{II}-O_2)$ frequency of HRP-III. On the other hand, in an oxidase, cleavage of the dioxygen bond is likely accomplished by adding electron density into the O=O bond, as this further populates the π^* orbital. Thus, in cytochrome oxidase intermediates, the dioxygen may assume a configuration that tends to build electron density between the oxygen atoms, resulting in a decrease in the $\nu(O=O)$ frequency and a concomitant increase in the $\nu(Fe^{II}-O_2)$ frequency. Our time-resolved studies, however, show that the initial Cyt Ox a_3—O_2 complex is relatively unperturbed by distal effects.[3] Thus, weakening and rupture of the O=O bond occurs in a subsequent step of the reaction.

Contribution from the Department of Chemistry,
Texas A&M University, College Station, Texas 77843-3255

Redox Chemistry of Iron Picolinate Complexes and of Their Hydrogen Peroxide and Dioxygen Adducts

Pablo Cofré, Silvia A. Richert, Andrzej Sobkowiak, and Donald T. Sawyer*

In aprotic solvents the bis(picolinato)iron(II) [Fe(PA)$_2$] and (2,6-pyridinedicarboxylato)iron(II) [Fe(DPA)] complexes react with hydrogen peroxide and with dioxygen to form a series of monooxygen and dioxygen intermediates and adducts [(PA)$_2$FeOFe(PA)$_2$ (1), (PA)$_2$Fe(OO), (PA)$_2$FeOFe(PA)$_2$·HOOH (2), and their analogues with Fe(DPA)]. The electron-transfer chemistries of the complexes and of their oxygenated products have been characterized by cyclic voltammetry, controlled-potential electrolysis, and rotated ring–disk voltammetry. These results in combination with UV–visible spectrophotometric and magnetic measurements have been used to develop a self-consistent mechanism for the formation of (PA)$_2$FeO(OO)Fe(PA)$_2$ (3) from (PA)$_2$FeOFe(PA)$_2$ (1) and HOOH and for its transformation of methylene carbons to ketones. In dimethylformamide, species 3 (formed from 1 and HOOH) spontaneously decomposes to singlet dioxygen ($^1O_2$) and 1.

The electron-transfer chemistry of transition-metal complexes in aprotic solvents has been of major interest for the past two decades, especially in relation to oxygen activation by metalloproteins. Because iron is the most common metal in such metalloenzymes, its mode of activation for HOOH and for O_2 via redox cycles of various iron complexes can provide insight into the catalytic mechanisms of oxidases, peroxidases, monooxygenases, and dioxygenases. The coordination complexes of iron(III) are prone to form μ-oxo-bridged dimers.[1-3] The mononuclear 8-quinolinol and 2-methyl-8-quinolinol complexes of iron(II) and -(III) react with molecular oxygen and hydrogen peroxide to form such μ-oxo dimers, which are catalytic for the decomposition of the superoxide ion.[4]

Related studies of manganese complexes as reaction mimics for the water oxidation cofactor in photosystem II indicate that the picolinate[5,6] and 2,6-pyridinedicarboxylate[7] ligands form especially rugged and relevant models for the manganese cofactor. When these ligands are coordinated to manganese, cobalt, and iron, they exhibit ligand-centered redox processes with redox potentials of +0.6 to −0.0 V vs NHE for the ML_3/ML_3^- process.[7,8] The tris(picolinato)manganese(III) complex facilitates the decomposition of hydrogen peroxide,[5] and the tris(picolinato)manganese(II) complex Mn(PA)$_2$(PAH)(H$_2$O) efficiently catalyzes the disproportionation of superoxide ion in acetonitrile or dimethyl sulfoxide[9] [as does the bis(8-quinolinolato)manganese(II) complex].[10] In aqueous media tris(picolinato)iron(II) catalyzes the decomposition of the superoxide ion via the generation of hydrogen peroxide and its iron-induced activation to produce hydroxyl radicals.[11]

(1) Ehman, D. L.; Sawyer, D. T. *Inorg. Chem.* **1969**, *8*, 900.
(2) Wilkins, R. G.; Yelin, R. E. *Inorg. Chem.* **1969**, *8*, 1470.
(3) Schugar, H. J.; Hubbard, A. T.; Anson, F. C.; Gray, H. B. *J. Am. Chem. Soc.* **1969**, *91*, 71.
(4) Seo, E. T.; Riechel, T. L.; Sawyer, D. T. *Inorg. Chem.* **1977**, *16*, 734.
(5) Yamaguchi, K.; Sawyer, D. T. *Inorg. Chem.* **1985**, *24*, 971.
(6) Matsushita, T.; Spencer, L.; Sawyer, D. T. *Inorg. Chem.* **1988**, *27*, 1167.
(7) Richert, S. A.; Tsang, P. K. S.; Sawyer, D. T. *Inorg. Chem.* **1988**, *27*, 1814.
(8) Richert, S. A.; Tsang, P. K. S.; Sawyer, D. T. *Inorg. Chem.* **1989**, *28*, 2471.
(9) Yamaguchi, K. S.; Spencer, L.; Sawyer, D. T. *FEBS Lett.* **1986**, *197*, 249.
(10) Howie, J. K.; Sawyer, D. T. *J. Am. Chem. Soc.* **1976**, *98*, 6698.
(11) Bannister, W. H.; Bannister, J. V.; Searle, A. J. F.; Thornalley, P. J. *Inorg. Chim. Acta* **1983**, *78*, 139.